photonics

MDPI

Review

Solid-State Color Centers for Single-Photon Generation

Greta Andrini [1,2,*], Francesco Amanti [3], Fabrizio Armani [4], Vittorio Bellani [5,6], Vincenzo Bonaiuto [7,8], Simone Cammarata [3,9], Matteo Campostrini [10], Thu Ha Dao [7,8], Fabio De Matteis [7,8], Valeria Demontis [6,11], Giovanni Di Giuseppe [12,13], Sviatoslav Ditalia Tchernij [2,14], Simone Donati [3,15], Andrea Fontana [6], Jacopo Forneris [2,14], Roberto Francini [7,8], Luca Frontini [4,16], Roberto Gunnella [12,13], Simone Iadanza [17], Ali Emre Kaplan [18], Cosimo Lacava [6,19], Valentino Liberali [4,16], Francesco Marzioni [12,13,20], Elena Nieto Hernández [2,14], Elena Pedreschi [3], Paolo Piergentili [12,13], Domenic Prete [6], Paolo Prosposito [7,8], Valentino Rigato [10], Carlo Roncolato [10], Francesco Rossella [6,21], Andrea Salamon [8], Matteo Salvato [8,22], Fausto Sargeni [8,23], Jafar Shojaii [24], Franco Spinella [3], Alberto Stabile [4,16], Alessandra Toncelli [3,15], Gabriella Trucco [6,25] and Valerio Vitali [6,19]

1 Dipartimento di Elettronica e Telecomunicazioni, Politecnico di Torino, 10129 Torino, Italy
2 INFN Sezione di Torino, 10125 Torino, Italy; sviatoslav.ditaliatchernij@unito.it (S.D.T.); jacopo.forneris@unito.it (J.F.); elena.nietohernandez@unito.it (E.N.H.)
3 INFN Sezione di Pisa, 56127 Pisa, Italy; francesco.amanti@pi.infn.it (F.A.); simone.cammarata@phd.unipi.it (S.C.); simone.donati@unipi.it (S.D.); elena.pedreschi@pi.infn.it (E.P.); franco.spinella@pi.infn.it (F.S.); alessandra.toncelli@unipi.it (A.T.)
4 INFN Sezione di Milano, 20133 Milano, Italy; luca.frontini@mi.infn.it (L.F.); valentino.liberali@mi.infn.it (V.L.); alberto.stabile@mi.infn.it (A.S.)
5 Dipartimento di Fisica, Università di Pavia, 27100 Pavia, Italy; vittorio.bellani@unipv.it
6 INFN Sezione di Pavia, 27100 Pavia, Italy; valeria.demontis@sns.it (V.D.); andrea.fontana@pv.infn.it (A.F.); cosimo.lacava@unipv.it (C.L.); domenic.prete@pv.infn.it (D.P.); francesco.rossella@unipv.it (F.R.); gabriella.trucco@unimi.it (G.T.); valerio.vitali@unipv.it (V.V.)
7 Dipartimento di Ingegneria Industriale, Università di Roma Tor Vergata, 00133 Roma, Italy; vincenzo.bonaiuto@uniroma2.it (V.B.); thuha.dao@students.uniroma2.eu (T.H.D.); dematteis@roma2.infn.it (F.D.M.); francini@roma2.infn.it (R.F.); paolo.prosposito@uniroma2.it (P.P.)
8 INFN Sezione di Roma Tor Vergata, 00133 Roma, Italy; andrea.salamon@roma2.infn.it (A.S.); matteo.salvato@roma2.infn.it (M.S.); fausto.sargeni@uniroma2.it (F.S.)
9 Dipartimento di Ingegneria dell'Informazione, Università di Pisa, 56122 Pisa, Italy
10 INFN Laboratori Nazionali di Legnaro, 35020 Legnaro, Italy; matteo.campostrini@lnl.infn.it (M.C.); valentino.rigato@lnl.infn.it (V.R.); carlo.roncolato@lnl.infn.it (C.R.)
11 NEST, Scuola Normale Superiore and Istituto Nanoscienze-CNR, 56127 Pisa, Italy
12 Scuola di Scienze e Tecnologie, Divisione di Fisica, Università di Camerino, 62032 Camerino, Italy; gianni.digiuseppe@unicam.it (G.D.G.); roberto.gunnella@unicam.it (R.G.); francesco.marzioni@unicam.it (F.M.); paolo.piergentili@unicam.it (P.P.)
13 INFN Sezione di Perugia, 06123 Perugia, Italy
14 Dipartimento di Fisica, Università di Torino, 10125 Torino, Italy
15 Dipartimento di Fisica, Università di Pisa, 56127 Pisa, Italy
16 Dipartimento di Fisica, Università di Milano, 20133 Milano, Italy
17 Paul Scherrer Institute, 5232 Villigen, Switzerland; simone.iadanza@psi.ch
18 Optoelectronics Research Center, University of Southampton, Southampton SO17 1BJ, UK; a.e.kaplan@soton.ac.uk
19 Dipartimento di Ingegneria Industriale e dell'Informazione, Università di Pavia, 27100 Pavia, Italy
20 Dipartimento di Fisica, Università di Napoli "Federico II", 80126 Napoli, Italy
21 Dipartimento di Scienze Fisiche, Informatiche e Matematiche, Università di Modena e Reggio Emilia, 41125 Modena, Italy
22 Dipartimento di Fisica, Università di Roma Tor Vergata, 00133 Roma, Italy
23 Dipartimento di Ingegneria Elettronica, Università di Roma Tor Vergata, 00133 Roma, Italy
24 Space Technology and Industry Institute, Swinburne University of Technology, Hawthorn, VIC 3122, Australia; jshojaii@swin.edu.au
25 Dipartimento di Informatica, Università di Milano, 20133 Milano, Italy
* Correspondence: greta.andrini@to.infn.it

Abstract: Single-photon sources are important for integrated photonics and quantum technologies, and can be used in quantum key distribution, quantum computing, and sensing. Color centers in the solid state are a promising candidate for the development of the next generation of single-photon

check for updates

Citation: Andrini, G.; Amanti, F.; Armani, F.; Bellani, V.; Bonaiuto, V.; Cammarata, S.; Campostrini, M.; Dao, T.H.; De Matteis, F.; Demontis, V.; et al. Solid-State Color Centers for Single-Photon Generation. *Photonics* **2024**, *11*, 188. https://doi.org/10.3390/photonics11020188

Received: 12 January 2024
Revised: 7 February 2024
Accepted: 10 February 2024
Published: 19 February 2024

sources integrated in quantum photonics devices. They are point defects in a crystal lattice that absorb and emit light at given wavelengths and can emit single photons with high efficiency. The landscape of color centers has changed abruptly in recent years, with the identification of a wider set of color centers and the emergence of new solid-state platforms for room-temperature single-photon generation. This review discusses the emerging material platforms hosting single-photon-emitting color centers, with an emphasis on their potential for the development of integrated optical circuits for quantum photonics.

Keywords: color centers; solid state; diamond; silicon carbide; hBN; nitrides; silicon semiconductor; single-photon source; integrated photonics

1. Introduction

Single-photon sources, i.e., physical systems offering the *on-demand* emission of individual photons with desired properties, are key ingredients for current and prospective applications in integrated photonics and quantum technologies [1]. In particular, the relevant properties that a single-photon source must have to enable the realization of these technologies generally include the photostable and on-demand delivery of fully polarized single indistinguishable photons. In addition, the ideal single-photon source is a scalable physical system operating at room temperature and characterized by a high emission count rate and quantum efficiency. The concept of single-photon sources originated in the late 20th century, with a significant subsequent body of work leading to their practical implementation. In the field of quantum communication, single-photon sources serve as building blocks for secure quantum key distribution (QKD) systems [2–4]. They also have the potential to play a pivotal role in quantum computing as optically addressable qubits for quantum information processing and sensing [5–7]. In the context of integrated photonics, these sources are also at the core of the development of quantum photonic circuits that integrate quantum components with existing optical technologies [8]. Although probabilistic sources based on approximating a quantum light emitter with attenuated lasers [9] or on nonlinear photon conversion processes [10,11] have gained immediate interest for high-level experiments in laboratory environments [12–14] and for selected commercial systems, the quest for deterministic sources exhibiting a truly on-demand behavior, with negligible multi-photon generation probability, has steadily led to the development of several alternative approaches, spanning cold atoms and ions [15], quantum dots [16,17], and isolated molecules [18]. Among the possible platforms, color centers in the solid state represent a viable candidate for the development of the next generation of single-photon sources integrated in quantum photonics devices. Color centers are point defects in a crystal lattice that absorb and emit light at given wavelengths, thus effectively acting as artificial atoms embedded in a solid-state material.

These unique quantum systems have immense potential as single-photon sources due to their ability to emit single photons with high efficiency, purity, and indistinguishability [19]. Furthermore, their occurrence as point defects at the solid state offers a viable path towards their native embedment in photonic circuits by micro- and nanofabrication of the host material. For several years, the interest in color centers has been limited to a few physical systems, among which, notably, is the nitrogen-vacancy center in diamond [20]. Due to sub-optimal emission properties for integrated photonics, scientific research has pursued specific applications such as the optically addressable spin properties for quantum sensing and computing. Since 2013, the landscape has changed abruptly with the subsequent identification of a wider set of color centers and the emergence of new, previously unexplored solid-state platforms for room-temperature-single-photon generation. In this review the most promising materials hosting single-photon-emitting color centers are discussed, with an emphasis on the perspective of their uptake for the development of integrated optical circuits for quantum photonics.

2. Single-Photon-Emitting Color Centers

Color centers are optically active defects that occur in the crystalline lattice structure of semiconductors and insulators. Both intrinsic, (i.e., related only to the occurrence of vacancies, interstitials, or their combination) and extrinsic (i.e., involving the presence of atomic impurities in the material) can result in optical transitions, depending on their specific electronic configuration. A color center presents an atom-like nature that is embedded in the solid-state matrix of the host material (Figure 1a). The structure can be described by a finite number of energy levels introduced in the forbidden gap, among which electron transitions are allowed (Figure 1b).

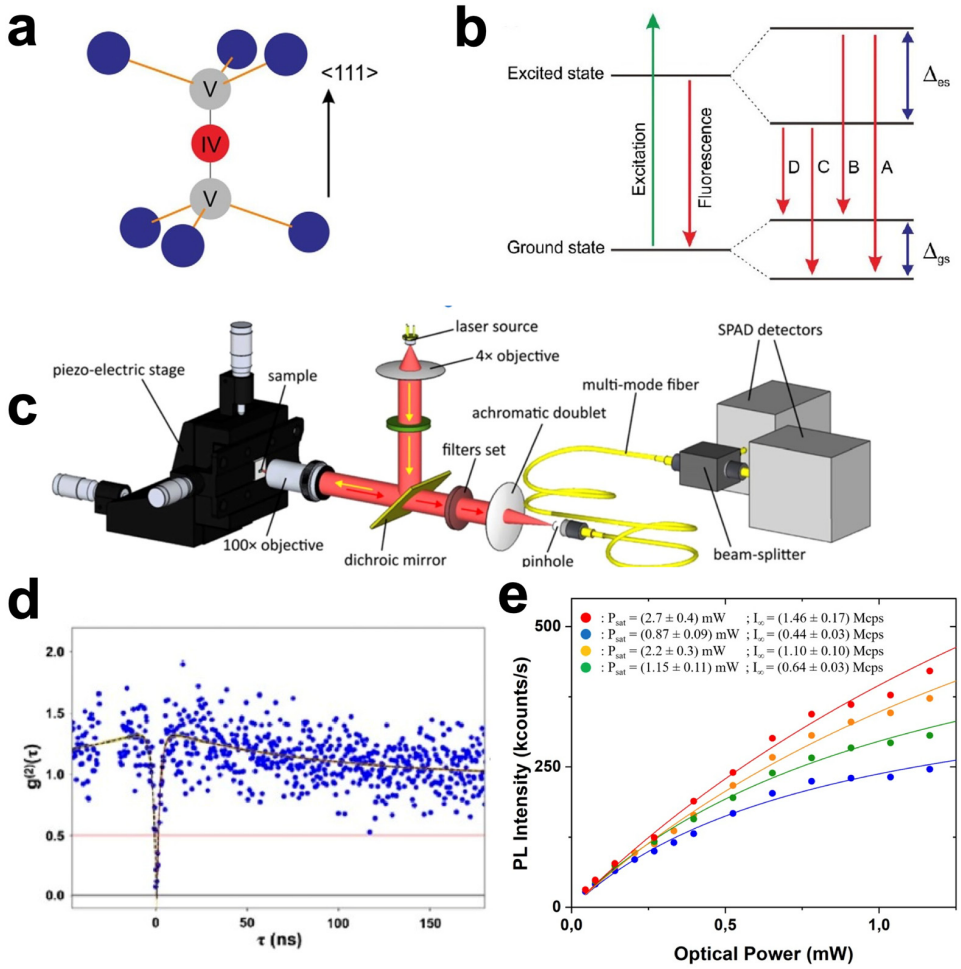

Figure 1. Color centers and experimental characterization. (**a**) Crystallographic structure and (**b**) fine-level structure of group IV color centers in diamond [21]. (**c**) Single-photon-sensitive confocal microscope connected to a Hanbury-Brown and Twiss interferometer [22]. (**d**) Example of a second-order autocorrelation function $g^2(\tau)$ measurement for a single MgV color center in diamond [23]. (**e**) Typical background-subtracted-emission–rate curves as a function of the optical excitation power for the saturation-intensity estimation according to the saturation model [23].

The electronic structure and related photon emission of a color center are typically discussed using a simplified model involving an excited state, a ground state, and generally a shelving state taking into account non-radiative transition paths, e.g., weakly allowed spin-flipping transitions from the excited state to the ground state [24] or resonant-energy-transfer processes involving neighboring lattice defects [25]. Therefore, the emission dynamics can be generally described using a two- or three-level system. The energy is delivered to the defect complex through the optical pumping of a laser pulse, while some color centers may also emit luminescence under electrical excitation [26]. The so-called

Zero Phonon Line (ZPL) indicates the emission wavelength of the emitted photons when the radiative transition occurs between ground-state vibrational levels. Conversely, the embedment of a point defect in a crystal lattice naturally involves the occurrence of phonon-assisted transitions. In this case, less energetic photons are emitted, populating the region of the emission spectrum commonly indicated as the phonon sideband. The fraction of light emitted in the ZPL with respect to the overall emission of the color center defines the Debye–Waller factor, a reference parameter to classify the eligibility of the source for the implementation of quantum computation schemes with matter qubits and linear optics [27]. Additionally, the linewidth of the ZPL provides a piece of benchmark information on the indistinguishability of the emitted photons. Figure 1c displays the single-photon-sensitive confocal microscope that is commonly adopted to study the optical properties of color centers [22]. Particularly, to discriminate the single-photon emission from thermal or coherent light, an analysis of the emission statistics is needed. A standard characterization technique is provided by the Hanbury-Brown and Twiss interferometer. This experimental method is implemented by feeding the light source onto a beam splitter separating the emission into two paths, each coupled to a single-photon-sensitive detector. Therefore, a time interferogram is obtained by acquiring a histogram of the differences between detection event pairs at the two detectors. In fact, under proper assumptions, the histogram of the time differences directly represents the so-called second-order autocorrelation function, $g^2(\tau)$, whose value at a zero-time delay is the main criterion used to measure the non-classicality of a source. Indeed, the emission collected from an ideal single-photon source will result in the lack of event pairs recorded at $\tau = 0$, producing an anti-bunching signature in the $g^2(\tau)$ histogram. The occurrence of nonclassical emission from an individual emitter is indeed verified when $g^2(0) < 0.5$ (Figure 1d). The $g^2(\tau)$ model for a three-level system is represented by a double-exponential function, in which the decay parameters are directly connected to the characteristic times associated with the de-excitation of the excited state and the shelving state [23]. As a result, the study of the second-order autocorrelation function is also a well-established procedure for evaluating the characteristic features of the transitions involved in the optical activity of the single emitter under study.

Moreover, since high-throughput information transmission and processing are needed in the practical implementation of quantum information processing devices such as QKD systems, the emission count rate is a key element for evaluating the suitability of the single-photon source for a given application. The emission intensity at saturation, meaning the maximum photon count rate when complete saturation of the emitter occurs, provides a reliable estimate of the source's brightness and, together with the corresponding optical power required for excitation, represents a useful quantitative parameter for the assessment of single-photon sources' performance. For instance, Figure 1e shows the emission count rate values for bright Mg-based single-photon sources in artificial diamond. Finally, the higher the emission probability after the defect's excitation, the higher the quantum efficiency of the single-photon emitter.

3. Material Platforms

3.1. Diamond

Artificial diamond has been a pioneering platform for single-photon generation in the solid state. The availability of point defects with optical transitions, known as color centers (Figure 2), is an established feature of the material due to intense room-temperature emission from a vast variety of defective complexes [28] (Table 1). The first demonstration of single-photon emission from a diamond color center was given in 2000 [29], based on an emitter consisting of the nitrogen-vacancy complex (NV center), namely a substitutional N atom coupled to a lattice vacancy. The NV center has gained increasing importance for the development of quantum-enhanced sensing and computing schemes due to its peculiar emission properties, enabling the optical initialization and readout of its spin state and its addressability by means of microwave fields [30–34]. Nevertheless, the large emission spectrum (575–800 nm range) due to a large interaction with the lattice phonons and its relatively low luminescence

intensity (<10^5 photons/s) pose significant limitations for the generation and manipulation of identical photons in integrated photonics circuits. These challenges shifted the interest of the scientific community towards alternative classes of diamond emitters with promising features, such as point defects based on group IV impurities [35]. Color centers based on Si (ZPL, at 738 nm) [36], Ge (602 nm) [37], Sn (620 nm) [38], and Pb (552 nm) [39] atoms share the same split-vacancy configuration and similar properties, such as a narrow emission line (Figure 2a), ~ns excited state lifetimes, Fourier-transform-limited emission, and an addressable ground-state splitting for quantum information processing [40–43]. Several additional emerging classes of interest are currently being explored in an attempt to map the optical activity of impurities incorporated in the diamond lattice, including the Mg-related-split-vacancy defects [23,44], the oxygen-related ST1 center [45], and noble gas impurities [46,47]. The main strength of these classes of color centers lies in their room-temperature operation, although there are unavoidable limitations in the degree of indistinguishability, and in their high photon emission rates (above 10^6 photons/s for several classes of defects [23,39,48]). Moreover, diamond color centers can be straightforwardly fabricated by means of the incorporation of selected impurities by ion implantation due to the relative simplicity of their defective structure, although their formation efficiency heavily depends on post-implantation activation processes [41,49–52]. Furthermore, laser writing has recently disclosed a novel approach in diamond-defect engineering for device fabrication, unlocking in-plane-high-spatial accuracy in the controlled placement of single emitters [51] and new perspectives for their integration in diamond chips [53].

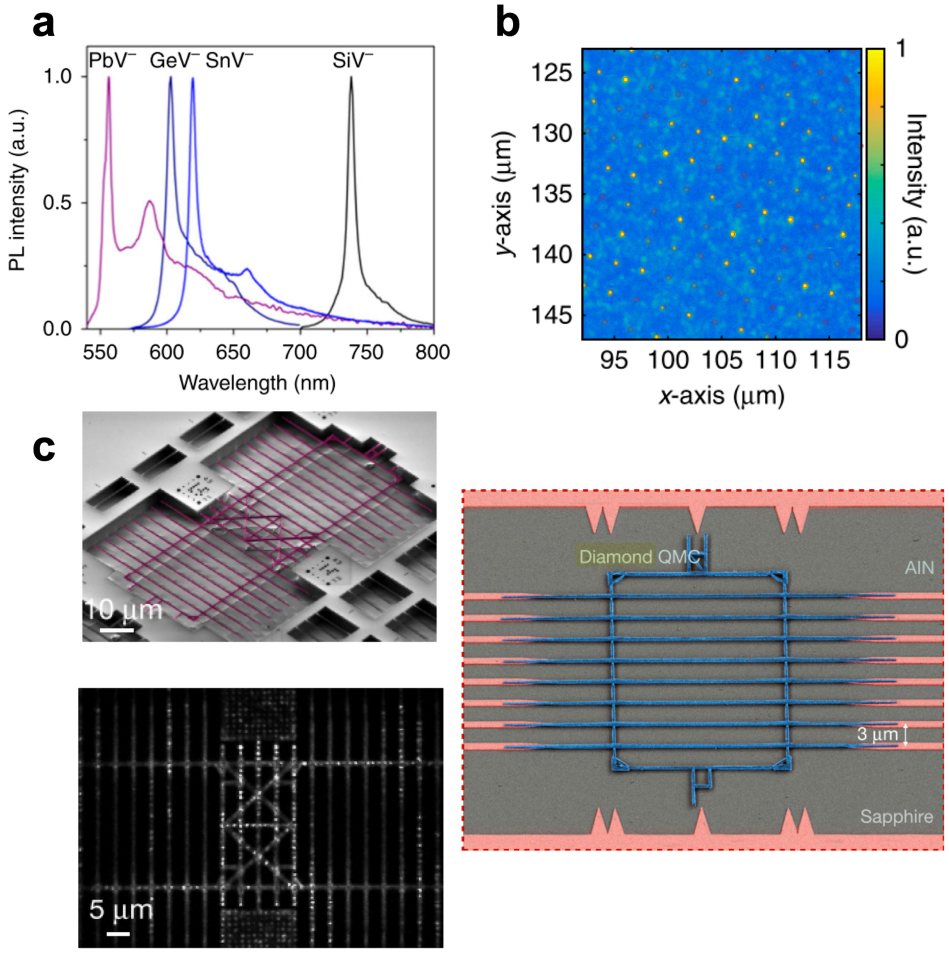

Figure 2. Color centers in diamond. (**a**) Photoluminescence emission spectra at room temperature from group IV impurities in diamond [35]. (**b**) Patterned nanoscale fabrication of SiV centers in diamond by means of focused-ion-beam implantation [54]. (**c**) Fabrication of hybrid photonic devices with integrated GeV color centers registered to diamond waveguides [55].

With respect to the doping of a diamond substrate with the desired atomic species during the chemical-vapor deposition or high-pressure–high-temperature synthesis of the material [56–58], ion implantation, possibly combined with high-power laser processing [59,60] has the advantage of delivering a controlled number of impurities at specific locations in the target crystal, with spatial accuracies below 100 nm (Figure 2b) [54,61]. This feature has enabled the demonstration of individual photon emitters coupled to waveguides and optical fibers [61–64], photonic crystals [65–68], and hybrid photonic circuits (Figure 2c) [55]. Conversely, the emission wavelength of the color centers explored so far in the scientific literature lie mostly in the visible range. The occurrence of emitters at telecom wavelengths will be crucial for the uptake of diamond-color-center technologies in integrated quantum photonics. Furthermore, despite some noteworthy achievements [26,69–71], the electrically insulating properties of diamond challenges the electrical excitation of single-photon emission from individual color centers, which would boost the integration of these systems in high-density-opto-electronic devices. To date, an external, optical excitation source is needed to trigger single-photon emission from individual point defects. Strategies for an efficient electrical excitation, paired with the future availability of a market-driven cost reduction for commercially available high-purity material, could pave the way towards diamond-based quantum photonics.

Table 1. Photophysical properties of SPs in diamond.

		ZPL (nm)	T (K)	Excited State Lifetime (ns)	FWHM at Operational Temperature (nm)	Single Emitter Saturation Count Rate (kcps)	Spin Manipulation	Integration of SPs with Photonic Structures	References
Diamond	NV	575, 638	RT	12–22	Broad emission	1 k	Yes	Yes	[19,30–34,61,65]
	SiV	738	RT	1.0–2.4	0.7–5	~4.8k	Yes	Yes	[35,54,55,62–64,66]
	GeV	602	RT	1.4–5.5	5	170–1.2 k	Yes	Yes	[35,37,52,55]
	SnV	620	RT	6	6	530	Yes	Yes	[35,38,67,68]
	PbV	520, 552	RT	>3	7	1.04 k			[35,39]
	MgV	558	RT	2.4	3	0.44–1.46 k			[23]
	ST1	557	RT	9		~5	Yes		[45]
	He	536, 560	RT	29, 106	<2 (ensemble)				[46]
	Xe	794, 812	RT	~0.77	Broad emission				[47]

3.2. Silicon Carbide

Silicon carbide (SiC) has recently gained relevance as a platform for room-temperature-solid-state-single-photon generation (Figure 3). As a diatomic compound containing silicon and carbon, SiC is a wide-bandgap semiconductor material offering similar optical properties and integrability in native photonic structures to diamond. Furthermore, it benefits from mature industrial-scale wafer growth and processing technology descending from the recent boost in commercial demand for power electronics [72]. Among the different available polytypes of the material, 4H- and 6H-SiC are those most adopted for point defect engineering.

The most studied defect class for single-photon generation in SiC is the Silicon-vacancy center (V_{Si}), a lattice defect characterized by the absence of a Si atom in its intended lattice site. Depending on the symmetry of the lattice site, the V_{Si} center can be found in two configurations corresponding to the occupation of the hexagonal or cubic lattice site of the polytype-packing layout [73]. For the 4H-SiC polytype, these two configurations are

associated with three different zero-phonon emission lines lying in the near-infrared region at 858.2 nm, 862 nm and 917 nm wavelengths [74–76], with optical transition lifetimes of the order of ~5 ns and emission intensity of ~10^4 photons/s [77]. The V_{Si} center also presents an electron spin number of 3/2 and 3 different ZPL in the NIR range, and it has been recently proposed as a novel sensor for quantum thermometry and magnetometry applications [77–82]. Also among the most appealing perspectives for the utilization of the V_{Si} center lies its addressability in the electroluminescence regime (Figure 3a) [83]. The manufacturability of SiC diodes by electrical doping of the material could enable, in perspective, the integration of single-photon sources in integrated photonic circuits without the need for external optical excitation sources and with a minimal amount of background-pump photons [84].

Another promising single-photon emitting defect is the Carbon anti-site–vacancy pair ($C_{Si}V_C$ center), consisting of a C atom occupying a Si lattice site (anti-site defect) coupled with a C vacancy [85]. This defect in its positive charge-state configuration [84] was the first isolated at the single-photon-emitter level in 4H-SiC in 2014, offering a single-photon emission at rates up to 2×10^6 photons/s [86]. Due to the lattice structure of SiC, this defect can be found in four non-equivalent configurations depending on the lattice sites occupied by the anti-site–vacancy pair, each corresponding to two different zero-phonon emission wavelengths in the 650–675 nm spectral range [74].

Both the V_{Si} and the $C_{Si}V_C$ centers are intrinsic defects, i.e., they do not require the introduction of external impurities in the SiC crystal lattice. Therefore, they can be fabricated simply by introducing radiation damage in the host crystal via the interaction with energetic ion [87–89], electron [90,91], or photon [92] beams. A subsequent high-temperature annealing is responsible for the formation of stable defective configuration in the crystal lattice. The occurrence of extrinsic color centers generated by the incorporation of external chemical species has been demonstrated so far only for a limited set of impurities [74], and the systematic investigation of the optical activity of impurity elements in SiC is still in progress. Noteworthy color centers fabricated upon ion implantation at the single-photon emitter level are the nitrogen-vacancy center (N_CV_{Si}), exhibiting single-photon emission in the telecom band (emission lines in the 1150–1350 nm range in 4H-SiC, depending on the configuration of the lattice site) with a 2 ns excited state lifetime [93,94], and the substitutional vanadium-related V4+ center (1279–1387 nm ZPLs, emission lifetime above 70 ns) [95]. These color centers, although displaying intriguing spin properties for quantum information processing at telecom wavelengths, are reported to offer emission rates of ~10^3 photons/s and ~10^2 photons/s, respectively. The low values of these rates constitute a potential limitation with respect to competing classes of color centers for high-throughput applications. As in the case of intrinsic defects, the emission wavelength of these defects depends on the considered lattice-stacking configuration of the point defect, which cannot be controlled a priori during the ion implantation process, ruled by the stochastic ion–lattice interaction [84]. Furthermore, the fabrication of desired defect classes is also challenged by the binary nature of the SiC compound. The formation of a specific point defect requires the location of specific atoms and vacancies at precise sites and anti-sites of the lattice, thus hindering a highly efficient formation yield and leaving room for the formation of undesired, optically active emitters.

Despite the material still having to reach full maturity for applications in quantum technologies, SiC has also been extensively explored as a potential host material for integrated photonics [96]. The efforts in the integration of color centers in monolithic SiC platforms have also recently resulted in the coupling of individual V_{Si} centers to solid-immersion lenses and nanopillars (Figure 3b) for photon-extraction-efficiency enhancement [90,97], resonant crystal cavities with Purcell enhancements up to a factor of 80 [98,99], and resonators for optical frequency conversion [100]. Table 2 summarize the photophysical properties of the discussed defects with single photon emission.

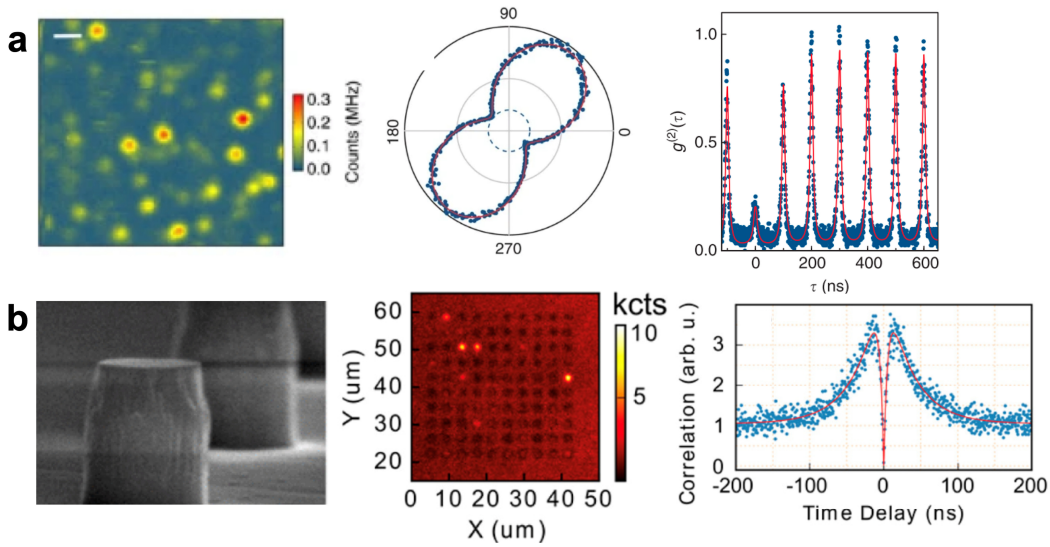

Figure 3. Color centers in silicon carbide. (**a**) Electrically stimulated single-photon emission from a $C_{Si}V_C$ center embedded in a SiC diode [83]. (**b**) Single V_{Si} centers registered to a high-density array of nanopillars fabricated by reactive ion etching [90].

Table 2. Photophysical properties of SPs in SiC.

		ZPL (nm)	T (K)	Excited State Lifetime (ns)	FWHM at Operational Temperature (nm)	Single Emitter Saturation Count Rate (kcps)	Spin Manipulation	Integration of SPs with Photonic Structures	References
Silicon Carbide	V_{Si}	858.2, 862, 917	RT	~5	<100	~10	Yes	Yes	[74–80,96]
	$C_{Si}V_C$	650–675	RT	1.2	>100	2 k			[74,84,86]
	NV	1150–1350	RT	2	1–3	17.4	Yes		[93,94]
	V4+	1279–1387	RT	>70			Yes		[95]

3.3. Silicon

Color centers in silicon offer an intriguing silicon-native alternative with respect to the aforementioned more consolidated classes of quantum emitters (Figure 4). Over the last few decades, despite its indirect band gap, silicon has shown the potential to integrate photon-emitting components with CMOS technology due to the occurrence of photoluminescence [101–103] and electroluminescence [104,105] from several optically active defects. However, the first demonstration of single-photon emission at cryogenic temperatures from a silicon point defect (the G center) was given only in 2020, kicking off a renewed interest in luminescent centers in silicon to develop next-generation technologies of the second quantum revolution [106].

The so-called G center consists of a bi-stable-dicarbon defective complex, whose neutral charge state is responsible for individual optical transitions at 1279 nm (0.97 eV) with emission intensity in the 10^4–10^5 photons/s range [106,107]. Theoretical calculations have revealed a fine structure of the ZPL with a splitting of ~2.5 μeV associated with the rotational levels of the interstitial silicon atom in the singlet excited state [108]. This rotational degree of freedom can be optically addressed in spinless, highly enriched ^{28}Si [109], thus removing the inhomogeneous broadening related to the heavier Si isotopes. In addition to the linewidth improvement, the G center possesses a metastable triplet state active under optically detected magnetic resonance [110], enabling appealing spin-selective singlet-triplet transitions for the implementation of a native qubit in silicon.

The demonstration of single-photon emission from the G center was rapidly followed by the study of additional classes of extrinsic and intrinsic defects emitting in the same spectral region (Table 3) [111–113], thus hinting at the availability of untapped resources for single-photon generation at telecom wavelengths. In particular, the T center, a defective complex consisting of two carbon atoms occupying a single silicon site, one of which is coupled to a hydrogen atom [114], was isolated at the single-photon emitter level in 2022 [115]. The latter provides another promising photon–spin interface with a ZPL emission at 1326 nm (0.94 eV), and long-lived electron and nuclear spin lifetimes (2 ms and 1.1 s, respectively [116]), offering spin-selective optical transitions at the telecom O band and a saturation intensity of 2 kcps [115]. On the other hand, it is characterized by a long radiative lifetime of the order of microseconds, and it is readily susceptible to dehydrogenation, requiring exact fabrication conditions [114].

An additional single-photon source of comparable brightness (2–6 kcps emission intensity at saturation) is the intrinsic complex known as W center, a tri-interstitial complex [117] that occurs as a typical radiation-induced defect in silicon [118–121]. As in the case of the G center [106], the photoluminescence emission from single W emitters is strongly polarized [117]. Finally, recent theoretical studies have uncovered the potential occurrence of already-studied carbon- and oxygen-related-radiation-damage defects called C centers [122,123] in implementing optically readable quantum memories [112]. Although their demonstration as single-photon sources is still unreported, the ZPL at 1570 nm (0.79 eV) experimentally observed at the ensemble level in irradiated Czochralski silicon samples [109,124,125] could pave the way for the implementation of telecom quantum networks, benefiting from minimal losses in commercial optical fibers.

The most apparent advantage of color centers compared to alternative strategies lies in their manufacturability by means of consolidated, industry-compatible fabrication and processing techniques, including ion implantation [107,111,126,127]. The same considerations made in the case of diamond hold for the controlled fabrication of quantum emitters with high spatial resolution and their registration to nanoscale photonic structures with minimal post-processing requirements. Progress in manufacturing strategies towards a controlled fabrication and placement of single-photon sources was shown for the G and W centers in focus ion beam technology with a spatial resolution below 100 nm (Figure 4a) [128].

Conversely, the viability of silicon color centers for integrated photonics might be challenged by the lack of tunability in the emission wavelengths of specific classes of color centers, combined with the current lack of emitters in the C-band range. Furthermore, single-photon emission in silicon has only been demonstrated at cryogenic temperatures so far, with a maximum temperature of 50 K [117]). The development of reliable methods for the manufacturing of individual color centers will also be crucial to their technological uptake. The available studies on the fabrication of the G center have pointed out how post-implantation thermal treatment can represent a limiting factor in realizing large-scale arrays of emitters, since it causes a broadening of the ZPL emission, which is a benchmark in the quality evaluation of the quantum source [129]. The emission broadening also exhibits a dependence on the ion implantation process itself, since broader emissions have been reported for carbon implantation [129] with respect to proton-irradiated samples [130].

The density of the fabricated G centers and the signal-to-noise ratios of individual emitters presented a direct connection with the annealing conditions as well [129], indicating a progressive dissociation of the defects alongside a decrease in the background signal for a longer annealing duration. Therefore, off-equilibrium fabrication strategies that involve dynamic annealing have been explored as a more valid alternative [130]. Particular care must be taken in how different thermal treatment durations used to supply the thermal budget can affect the evolution and stabilization of the G center with respect to competing defective complexes. Proof of this lies in the lower temperature reported for the annealing out of the W (~400 °C [111,131,132] and G center (~250 °C [101]) following conventional rapid thermal annealing and compared to the peak temperature estimated in ns-pulsed ion implantation [133]. Non-equilibrium processes with μs-long high-power laser exposure

combined with surface functionalization based on organic molecules have also promoted the incorporation of carbon atoms above the solubility limit, thus creating a highly dense ensemble of G centers [105].

On the other hand, in the direction of single-defect engineering, more responsive thermal processing has been explored in C-implanted float zone silicon, investigating localized heating effects upon non-invasive ns-pulsed laser annealing [134]. In addition to this, ensemble G and W emission signal has been reported upon femtosecond laser-induced melting and recrystallisation of silicon [135], with results in agreement with earlier studies on the solid-phase annealing of carbon-implanted silicon in proximity to the laser-melted region [136,137].

When integrating single-photon emitters into photonic structures, considering how different fabrication processes affect the inhomogeneous broadening and other quality parameters of the source becomes highly relevant to realizing the required experimental conditions, such as the spatial and spectral overlapping between the single defect and the nanocavity. For instance, strain engineering has provided a useful method to tune the splitting of the G center ZPL in doublets or quadlets up to 18 meV [138], and particular attention has been paid to avoiding the introduction of unwanted radiation-related defects while developing nanopatterning processes to integrate these sources in photonic platforms [139]. In addition, a 30-fold enhancement of the photoluminescence coming from single G emitters and an 8-fold Purcell enhancement of their emission rate has been recently achieved in an all-silicon cavity [133]. Cryogenic temperatures do not necessarily represent a practical limitation in the photonic circuit integration, where low-temperature conditions are already required; for instance, for the integration of superconducting nanowire single-photon detectors. Waveguide-coupled emission coming from ensembles of W centers fabricated in the intrinsic region of an electrically injected LED has indeed been reported in an all-silicon-integrated chip [140]. On the other hand, free space optical pumping of W defects whose PL signal has been coupled to an SOI waveguide and microring resonators has been more recently achieved, with the advantage with of more relaxed fabrication and operational requirements [141]. Despite the need for the controlled fabrication and positioning of individual color centers, which are still crucial challenges in building large-scale integrated quantum photonics silicon platforms, significant advances, such as the monolithic integration of a single G center into a single-mode waveguide operating at its ZPL (Figure 4b) [142], have once more stressed the potentiality in utilizing these systems for quantum information processing.

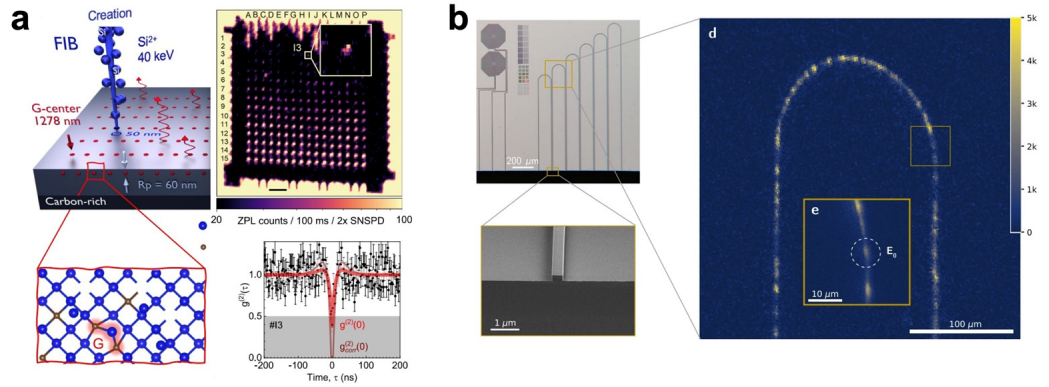

Figure 4. Color centers in silicon. (**a**) Nanofabrication and detection of single-photon emitters in silicon using focused ion beams (FIB) [128]. (**b**) Integration of individual G centers in a silicon-on-insulator photonic integrated circuit platform [142].

Table 3. Photophysical properties of SPs in Silicon.

		ZPL (nm)	T (K)	Excited State Lifetime (ns)	FWHM at Operational Temperature (nm)	Single Emitter Saturation Count Rate (kcps)	Spin Manipulation	Integration of SPs with Photonic Structures	References
Silicon	G	1279	4–110 K	35.8	0.28	8	Yes	Yes	[103,106,110, 131,142]
	W	1218	4–60 K	3–34.5	0.1	2–6		Yes	[111,117,140, 141]
	T	1326	<5 K	940	0.04	2	Yes		[115,116]

3.4. Nitrides

Among emerging platforms for solid-state-single-photon generation, nitride materials [143,144] stand out because of their already mature fabrication process, as in the case of GaN or SiN [145,146], and their consolidated utilization in integrated photonics, especially for waveguides and other photonic structures in SiN [147] (Figure 5). Table 4 summarize the photophysical properties of the defects with single photon emission in nitride materials.

Gallium Nitride (GaN) was the first bulk nitride platform to be reported to host single-photon sources. GaN is a direct-wide-bandgap (3.45 eV) semiconductor employed in the past few decades mainly as a platform for LEDs operating across the whole visible spectrum [148] and in high-power electronics. The material also received attention for the development of photonics structures and optoelectronics at the nanoscale [143,149–151], indicating a high degree of maturity for the uptake of single-photon sources in integrated devices. The first report on single-photon sources in GaN dates back to 2017 [152,153] with the discovery of a class of native single-photon emitters. The emission was denoted by a sharp ZPL with a large emitter-dependent variability in the 600–700 nm spectral range [152,153], exhibiting an ~ns excited state lifetime and high room-temperature emission intensity at saturation (1–5 $\times$ 10^5 photons/s). The integration of these emitters in photonic structures [154,155] and GaN substrates' layered growth [156] has followed. An additional class of bright color centers emitting single photons at telecom wavelengths (1100–1300 nm) was also identified in 2018 [157]. These emitters operate at room temperature with rates up to 5 $\times$ 10^5 photons/s and have been integrated into photonic structures for further emission enhancement [157,158]. Conversely, the reported classes of emitters were found natively in GaN and their unambiguous attribution to a specific defective complex is still missing, thus currently limiting the perspective of a controlled fabrication process for integration in quantum photonic circuits.

Aluminum Nitride (AlN) is a wide-bandgap semiconductor (Eg = 6.03 eV) that is widely employed as a piezoelectric material and in high-power electronics. It is also exploited in photonics as a substrate layer for the growth of GaN [159]. The first experimental demonstration of single-photon emission in AlN was reported in 2020 [160–162] from native defects. Individual defects were identified in thin AlN films grown on a sapphire substrate, and they exhibited room-temperature-linear-polarized emission from the visible to the infrared (550–1000 nm) range, with count rates up to 5 $\times$ 10^5 photons/s and a 2–3 ns excited state lifetime. The nature of these emitters has not been attributed in a conclusive manner as yet. The observed emission lines could be related to different classes of color centers or different site symmetries of the same point defect. Conversely, the large spectral variability observed in the literature could originate from the interaction with the crystal lattice environment in a piezoelectric material. Recent work has shown the role of Al-ion implantation and subsequent thermal annealing up to 600 °C in the formation of individual color centers in the 550–650 nm range, indicating that their structural configuration can be achieved by the controlled introduction of radiation-induced lattice damage and thus offering a convenient pathway for their manufacturing [163]. Such findings are in line with the demonstration of the deterministic fabrication of single color centers by fs laser-induced

damage in AlN on sapphire films [164]. These results, along with the theoretical prediction of point defects with optically addressable spin properties, similar to those of the NV center in diamond [165], highlight the potentially seamless integration of AlN emitters into integrated platforms for quantum photonics [166,167]. The efficient registration of single-photon sources into integrated circuits has already been proved in 2020 with the integration of a quantum emitter into a waveguide by means of grating couplers (Figure 5a) [168].

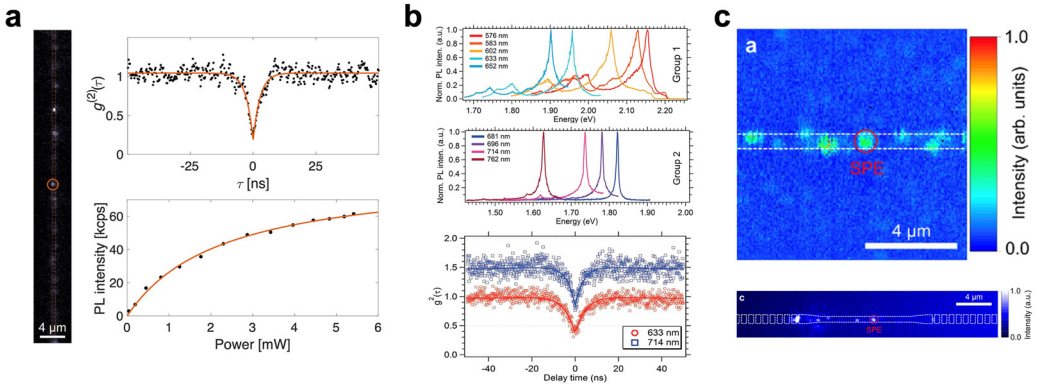

Figure 5. Color centers in nitrides. (**a**) Bright emitters from AlN point defects embedded in a waveguide [168]. (**b**) Variability in the emission wavelength from defective complexes in hBN [169]. (**c**) Coupling of native color centers in a SiN waveguide [170].

Hexagonal boron nitride (hBN) possesses the outstanding feature of being a 2-dimensional wide-bandgap semiconductor (~6 eV). The first demonstration of single-photon emitters at 623 nm in hBN dates back to 2016 [171] and was tentatively assigned to the V_NN_B anti-site-nitrogen-vacancy center [171–173]. The material has since attracted increasing attention with the identification of several classes of optically active defects filling the whole visible spectrum up to 850 nm [174,175]. Among the emitting defects, the ZPL at 630 nm has been attributed to the carbon–nitrogen-vacancy complex V_BC_N [176]. Conversely, the negatively charged boron vacancy V_B^- is responsible for the broad light emission at 850 nm. This latter defect has demonstrated optical-spin properties similar to those of the NV center in diamond, making it one of the few spin defects optically addressable at room temperature [175,177,178]. The main strengths of hBN-based single-photon sources lie in their reliable emission from cryogenic temperatures up to 800 K, emission rates above 4×10^6 photons/s, strongly polarized emission, strain-tunable emission wavelength (Figure 5b), and Fourier-transform-limited emission at room temperature [169,171,179–181]. The localized fabrication of emitters in hBN has been achieved so far with a variety of experimental methods [182], including thermal annealing [169], plasma treatment [183], femtosecond-pulsed laser [184,185], electron [169,186] and particle irradiations [187,188], and strain field engineering [180,189]. These results, in parallel with significant efforts to shed light on the structural nature of the discussed classes of emitters [190], indicate the readiness of the material for the scalable fabrication of arrays of quantum emitters. Furthermore, the coupling of hBN single-photon emitters in a wide variety of hybrid photonic structures has been explored extensively in the last years to both connect the generated photons with external circuits and to provide a higher collection efficiency. The integrability of the material is eased by its 2-dimensional structures, which enable in situ growth or deterministic placing of hBN flakes [191]. Preliminary demonstrations include the coupling to waveguides [192,193], microresonators [144], crystal cavities [194–196], antennas [197] and integrated photonic chips [198,199].

Silicon Nitride (SiN) is among the most used materials for the fabrication of integrated photonic circuits [200,201], both because of its low optical losses and its suitability for nonlinear photonics and microwave photonics [202–204]. Although hybrid single-photon generation systems have been developed by interfacing quantum dots [146] and hBN emitters [144] with SiN waveguides, the occurrence of quantum emitters related to native

defects has been demonstrated in 2021 [205] in SiN produced by chemical-vapor-deposition growth on SiO_2-coated silicon substrate and subsequent thermal annealing. These color centers are denoted by a linearly polarized emission distributed at four wavelengths in the 567–670 nm spectral range. Room-temperature-single-photon-emission intensity can achieve 5×10^5 photons/s at saturation. This demonstration was immediately followed by the integration of native SiN emitters in all-SiN waveguides (Figure 5c) [170]. The research on these systems is at its infancy and a clear attribution of the defective structure of the reported color centers has yet to be obtained, as in the case of GaN and AlN emitters. Nonetheless, they are indicative of appealing perspectives towards the implementation of integrated, monolithic photonic chips with integrated, native single-photon sources.

Table 4. Photophysical properties of SPs in Nitrides.

		ZPL (nm)	T (K)	Excited State Lifetime (ns)	FWHM at Operational Temperature (nm)	Single Emitter Saturation Count Rate (kcps)	Spin Manipulation	Integration of SPs with Photonic Structures	References
(Mg)-doped and undoped GaN films	Intrinsic defects	600–700	RT	~1–3	~5	100–150		Yes	[152–155]
	Intrinsic defects	1100–1300	RT	0.7	3–50	500		Yes	[157,158]
AlN	$N_{Al}V_N$, $V_{Al}V_N$	550–1000	RT	~2	<12	500		Yes	[161,162,168]
hBN	V_NN_B	623	RT	~3		>4 k		Yes (without attribution to a specific defect complex)	[171–173,179–181]
	V_BC_N	630	RT	~2–6	~5–35	>4 k			[171,176,179–181,191–197]
	V_B^-	850	RT	1.2	Broad emission	>4 k	Yes		[169,175,177–181]
SiN	Intrinsic defects	567–670	RT	3.8	Broad emission	500		Yes	[170]

4. Perspectives

The quest for optimal classes of solid-state color centers and their integration in integrated quantum photonics platforms is a buzzing research field that has achieved impressive developments in the last decade. Several quantum systems have been demonstrated in different materials, each offering peculiar properties and advantages combined with specific limitations. From the point of view of the maturity of each considered material as a platform for integrated quantum photonics, different challenges are still to be addressed. However, depending on the specific quantum protocol to be implemented, the availability of color centers with different emission properties allow one to identify a suitable trade-off between the manufacturing opportunities and the accompanying drawbacks. For instance, quantum-enhanced sensing protocols require the optical addressability of the spin system and its coherent manipulation, without the strict need for high-indistinguishability or NIR/IR emission wavelengths. Conversely, the development of quantum-integrated photonic circuits requires a hyperfine coupling with nearby nuclear spins as a key parameter for transferring quantum information between the electron spin of the quantum emitters and the proximate nuclear spins of the crystal environment. Furthermore, the realization of solid-state quantum memories does not necessarily find its limitation in the VIS emission wavelengths when long-distance communication is not demanded. If the realization of larger programmable photonic processors is targeted [206], i.e., characterized by a large number of qubits and thus capable of processing higher complexity algorithms, industry-scale-compatible manufacturing processes could be beneficial together with a consolidated

maturity of the material platform synthesis (e.g., silicon CMOS technology). Moreover, if the emitted single photons are intended to be used in quantum processing systems based on commercial optical fibers, the emission in the telecom band represents an important prerequisite to minimize the losses. On the other hand, indistinguishable photons constitute the prerequisite for quantum interference effects underpinning the linear quantum optics paradigm [19,207]; consequently, the availability of solid-state single-photon emitters with Fourier-transform-limited emission lines is crucial for this range of applications.

Artificial diamond has been the pioneering material for the development of color centers, partly due to its defectivity. Significant progress in the material synthesis field has been achieved since the discovery of the first quantum emitter in 2000, and high-purity crystals are routinely available on the market, although in sizes not exceeding a few millimeters. The relative scarcity of competing manufacturers is still limiting the development of this research field due to the large costs of bulk samples with respect to the alternative solid-state platforms. Conversely, an ample commercial availability of nanodiamond powders derived from industrial usage [208] is boosting the research in quantum sensing at the nanoscale [209,210]. This approach could be exploited to develop hybrid photonic platforms integrating single-photon sources embedded in nanodiamonds [211,212]. The fabrication by means of ion implantation has been amply demonstrated for several classes of diamond color centers. Diamond is currently the only material for which an extensive scientific literature is available on the optimization of the formation yield of color centers by several approaches, spanning from surface chemical functionalization [213] to co-doping [49] and post-implantation processes [52].

Silicon carbide is among the most mature platforms from the point of view of the material's synthesis, with commercially available wafer-scale-high-purity substrates and consolidated utilization for electronics and optoelectronics industrial applications [72]. On the other hand, the controlled fabrication of desired classes of color centers is hindered by the binary nature of the compound and the different stacking configurations available for each structural defect, and only few works have explored the integration of SiC color centers in photonic structures.

Silicon is certainly the most mature material in terms of synthesis and device manufacturing, as it relies on decades of expertise in research and industry. Conversely, the classes of color centers identified so far exhibit a molecular lattice structure substantially different from the simpler impurity–vacancy configurations found in diamond and SiC [108,114]. This peculiar feature challenges the consistent and repeatable fabrication of individual color centers by means of standard fabrication techniques such as ion implantation. Identifying suitable pathways for the high-yield production of single-photon sources is among the most compelling of needs.

The discovery of single-photon sources in bulk nitrides is very recent. Consequently, a clear understanding of the structural nature of the currently known classes of color centers is still missing and it will be crucial to open the path towards their controlled fabrication. Significant progress in the understanding of color centers in hBN has been recently made in terms of the control and engineering of emitters. This versatility, partly relying on a general understanding of the properties of 2-dimensional materials derived from the extensive investigation of graphene in the last two decades [214], make the hBN a compelling candidate for the development of integrated, although hybrid, quantum photonics.

Concerning the emergence of optimal classes of color centers for quantum information processing in integrated photonics circuits, the large availability of systems available at the solid state comes with its own set of promises to be developed and challenges to be overcome. The vast majority of the single-photon sources identified is associated with emission in the visible range. This is arguably a consequence of technological and instrumental contingencies, such as the commercial availability of single-photon detectors with high efficiency and affordable costs in this sole spectral range. It is, however, worth mentioning that new-generation-single-photon detectors with high efficiency at telecom wavelengths started to hit the market in recent years, based on superconducting systems

such as the SNSPD (superconducting nanowire single-photon detectors) [215]. These systems are still significantly more expensive than their solid-state-based counterparts due to the need for cryogenic operation, and their integration in confocal photoluminescence microscopes is marginal. Nonetheless, the technological leap will enable an extended investigation of the most promising solid-state platforms for the identification of telecom emitters tailored to specific applications.

As a last challenge for the uptake of solid-state color centers in integrated quantum photonics, the indistinguishability of the emitted photons will enable the implementation of quantum information processing operations based on entangled pairs [12,19,207] generated from a deterministic source. The achievement of a high degree of photon indistinguishability is among the biggest challenges for solid-state color centers, due to their coupling with the host lattice, external fields, and local inhomogeneities. For these reasons, this goal, or at least the occurrence of Fourier-transform limited photon emission [216] has been demonstrated for few classes of emitters so far, and it was typically achieved at cryogenic temperatures [40,78,217], with the notable exception of the V_NN_B center in hBN [181]. Different sources of spectral line broadening must be carefully identified, prevented, or counteracted in the fabrication of the emitters and in the design of the integrated quantum photonic circuits.

Author Contributions: All authors contributed to this work. Writing—original draft preparation, G.A., J.F. and E.N.H.; writing—review and editing, all authors. All authors have read and agreed to the published version of the manuscript.

Funding: This work has been funded by INFN through the CSN5 QUANTEP.

Acknowledgments: V.Be.: G.D.G., A.F., R.G., C.L., E.P., P. Pi., V.R., C.R., A.Sa and F.Sp. acknowledge the support of PNRR MUR project PE0000023-NQSTI (Italy). J.F. acknowledges the support of the 20IND05 (QADeT) that has received funding from the EMPIR program co-financed by the Participating States and from the European Union's Horizon 2020 research and innovation program. E.N.H. acknowledges the support of the ERC project "Training on LASer fabrication and ION implantation of DEFects as quantum emitters" (LasIonDef) funded under the "Marie Skłodowska-Curie Innovative Training Networks" program.

Conflicts of Interest: The authors declare no conflicts of interest.

References

1. Eisaman, M.D.; Fan, J.; Migdall, A.; Polyakov, S.V. Invited Review Article: Single-photon sources and detectors. *Rev. Sci. Instrum.* **2011**, *82*, 071101. [CrossRef]
2. Takemoto, K.; Nambu, Y.; Miyazawa, T.; Sakuma, Y.; Yamamoto, T.; Yorozu, S.; Arakawa, Y. Quantum key distribution over 120 km using ultrahigh purity single-photon source and superconducting single-photon detectors. *Sci. Rep.* **2015**, *5*, 14383. [CrossRef]
3. Leifgen, M.; Schröder, T.; Gädeke, F.; Riemann, R.; Métillon, V.; Neu, E.; Hepp, C.; Arend, C.; Becher, C.; Lauritsen, K.; et al. Evaluation of nitrogen- and silicon-vacancy defect centres as single photon sources in quantum key distribution. *New J. Phys.* **2014**, *16*, 023021. [CrossRef]
4. Schiavon, M.; Vallone, G.; Ticozzi, F.; Villoresi, P. Heralded single-photon sources for quantum-key-distribution applications. *Phys. Rev. A* **2016**, *93*, 012331. [CrossRef]
5. Awschalom, D.D.; Hanson, R.; Wrachtrup, J.; Zhou, B.B. Quantum technologies with optically interfaced solid-state spins. *Nat. Photonics* **2018**, *12*, 516–527. [CrossRef]
6. Piergentili, P.; Amanti, F.; Andrini, G.; Armani, F.; Bellani, V.; Bonaiuto, V.; Cammarata, S.; Campostrini, M.; Cornia, S.; Dao, T.H.; et al. Quantum Information with Integrated Photonics. *Appl. Sci.* **2023**, *14*, 387. [CrossRef]
7. Polino, E.; Valeri, M.; Spagnolo, N.; Sciarrino, F. Photonic quantum metrology. *AVS Quantum Sci.* **2020**, *2*, 024703. [CrossRef]
8. Wang, J.; Sciarrino, F.; Laing, A.; Thompson, M.G. Integrated photonic quantum technologies. *Nat. Photonics* **2020**, *14*, 273–284. [CrossRef]
9. Paraïso, T.K.; Woodward, R.I.; Marangon, D.G.; Lovic, V.; Yuan, Z.; Shields, A.J. Advanced Laser Technology for Quantum Communications (Tutorial Review). *Adv. Quantum Technol.* **2021**, *4*, 2100062. [CrossRef]
10. Li, X.; Voss, P.L.; Sharping, J.E.; Kumar, P. Optical-Fiber Source of Polarization-Entangled Photons in the 1550 nm Telecom Band. *Phys. Rev. Lett.* **2005**, *94*, 053601. [CrossRef] [PubMed]
11. Signorini, S.; Pavesi, L. On-chip heralded single photon sources. *AVS Quantum Sci.* **2020**, *2*, 041701. [CrossRef]

12. Broome, M.A.; Fedrizzi, A.; Rahimi-Keshari, S.; Dove, J.; Aaronson, S.; Ralph, T.C.; White, A.G. Photonic Boson Sampling in a Tunable Circuit. *Science* **2013**, *339*, 794–798. [CrossRef] [PubMed]
13. Adcock, J.C.; Vigliar, C.; Santagati, R.; Silverstone, J.W.; Thompson, M.G. Programmable four-photon graph states on a silicon chip. *Nat. Commun.* **2019**, *10*, 3528. [CrossRef] [PubMed]
14. Hu, X.-M.; Guo, Y.; Liu, B.-H.; Li, C.-F.; Guo, G.-C. Progress in quantum teleportation. *Nat. Rev. Phys.* **2023**, *5*, 339–353. [CrossRef]
15. Kuhn, A.; Hennrich, M.; Rempe, G. Deterministic Single-Photon Source for Distributed Quantum Networking. *Phys. Rev. Lett.* **2002**, *89*, 067901. [CrossRef] [PubMed]
16. Norman, J.C.; Jung, D.; Wan, Y.; Bowers, J.E. Perspective: The future of quantum dot photonic integrated circuits. *APL Photon.* **2018**, *3*, 030901. [CrossRef]
17. Arakawa, Y.; Holmes, M.J. Progress in quantum-dot single photon sources for quantum information technologies: A broad spectrum overview. *Appl. Phys. Rev.* **2020**, *7*, 021309. [CrossRef]
18. Toninelli, C.; Gerhardt, I.; Clark, A.S.; Reserbat-Plantey, A.; Götzinger, S.; Ristanović, Z.; Colautti, M.; Lombardi, P.; Major, K.D.; Deperasińska, I.; et al. Single organic molecules for photonic quantum technologies. *Nat. Mater.* **2021**, *20*, 1615–1628. [CrossRef]
19. Aharonovich, I.; Englund, D.; Toth, M. Solid-state single-photon emitters. *Nat. Photonics* **2016**, *10*, 631–641. [CrossRef]
20. Schirhagl, R.; Chang, K.; Loretz, M.; Degen, C.L. Nitrogen-Vacancy Centers in Diamond: Nanoscale Sensors for Physics and Biology. *Annu. Rev. Phys. Chem.* **2014**, *65*, 83–105. [CrossRef] [PubMed]
21. Iwasaki, T. Color centers based on heavy group-IV elements. *Semicond. Semimet.* **2020**, *103*, 237. [CrossRef]
22. Gatto Monticone, D.; Traina, P.; Moreva, E.; Forneris, J.; Olivero, P.; Degiovanni, I.P.; Taccetti, F.; Giuntini, L.; Brida, G.; Amato, G.; et al. Native NIR-emitting single colour centres in CVD diamond. *New J. Phys.* **2014**, *16*, 053005. [CrossRef]
23. Corte, E.; Andrini, G.; Nieto Hernández, E.; Pugliese, V.; Costa, Â.; Magchiels, G.; Moens, J.; Tunhuma, S.M.; Villarreal, R.; Pereira, L.M.C.; et al. Magnesium-Vacancy Optical Centers in Diamond. *ACS Photonics* **2023**, *10*, 101–110. [CrossRef]
24. Doherty, M.W.; Manson, N.B.; Delaney, P.; Jelezko, F.; Wrachtrup, J.; Hollenberg, L.C. The nitrogen-vacancy colour centre in diamond. *Phys. Rep.* **2013**, *528*, 1–45. [CrossRef]
25. Siyushev, P.; Jacques, V.; Aharonovich, I.; Kaiser, F.; Müller, T.; Lombez, L.; Atatüre, M.; Castelletto, S.; Prawer, S.; Jelezko, F.; et al. Low-temperature optical characterization of a near-infrared single-photon emitter in nanodiamonds. *New J. Phys.* **2009**, *11*, 113029. [CrossRef]
26. Forneris, J.; Traina, P.; Gatto Monticone, D.; Amato, G.; Boarino, L.; Brida, G.; Degiovanni, I.P.; Enrico, E.; Moreva, E.; Grilj, V.; et al. Electrical stimulation of non-classical photon emission from diamond color centers by means of sub-superficial graphitic electrodes. *Sci. Rep.* **2015**, *5*, 15901. [CrossRef]
27. Martínez, J.A.; Parker, R.A.; Chen, K.C.; Purser, C.M.; Li, L.; Michaels, C.P.; Stramma, A.M.; Debroux, R.; Harris, I.B.; Appel, M.H.; et al. Photonic Indistinguishability of the Tin-Vacancy Center in Nanostructured Diamond. *Phys. Rev. Lett.* **2022**, *129*, 173603. [CrossRef]
28. Zaitsev, A.M. *Optical Properties of Diamond*; Springer: New York, NY, USA, 2001.
29. Brouri, R.; Beveratos, A.; Poizat, J.-P.; Grangier, P. Photon antibunching in the fluorescence of individual color centers in diamond. *Opt. Lett.* **2000**, *25*, 1294–1296. [CrossRef]
30. Ruf, M.; Wan, N.H.; Choi, H.; Englund, D.; Hanson, R. Quantum networks based on color centers in diamond. *J. Appl. Phys.* **2021**, *130*, 070901. [CrossRef]
31. Pezzagna, S.; Meijer, J. Quantum computer based on color centers in diamond. *Appl. Phys. Rev.* **2021**, *8*, 011308. [CrossRef]
32. Barton, J.; Gulka, M.; Tarabek, J.; Mindarava, Y.L.; Wang, Z.; Schimer, J.; Raabova, H.; Bednar, J.; Plenio, M.B.; Jelezko, F.; et al. Nanoscale Dynamic Readout of a Chemical Redox Process Using Radicals Coupled with Nitrogen-Vacancy Centers in Nanodiamonds. *ACS Nano* **2020**, *14*, 12938–12950. [CrossRef]
33. Bourgeois, E.; Gulka, M.; Nesladek, M. Photoelectric Detection and Quantum Readout of Nitrogen-Vacancy Center Spin States in Diamond. *Adv. Opt. Mater.* **2020**, *8*, 1902132. [CrossRef]
34. Webb, J.L.; Troise, L.; Hansen, N.W.; Frellsen, L.F.; Osterkamp, C.; Jelezko, F.; Jankuhn, S.; Meijer, J.; Berg-Sørensen, K.; Perrier, J.-F.; et al. High-Speed Wide-Field Imaging of Microcircuitry Using Nitrogen Vacancies in Diamond. *Phys. Rev. Appl.* **2022**, *17*, 064051. [CrossRef]
35. Bradac, C.; Gao, W.; Forneris, J.; Trusheim, M.E.; Aharonovich, I. Quantum nanophotonics with group IV defects in diamond. *Nat. Commun.* **2019**, *10*, 5625. [CrossRef] [PubMed]
36. Wang, C.; Kurtsiefer, C.; Weinfurter, H.; Burchard, B. Single photon emission from SiV centres in diamond produced by ion implantation. *J. Phys. B* **2006**, *39*, 37–41. [CrossRef]
37. Iwasaki, T.; Ishibashi, F.; Miyamoto, Y.; Doi, Y.; Kobayashi, S.; Miyazaki, T.; Tahara, K.; Jahnke, K.D.; Rogers, L.J.; Naydenov, B.; et al. Germanium-Vacancy Single Color Centers in Diamond. *Sci. Rep.* **2015**, *5*, 12882. [CrossRef] [PubMed]
38. Iwasaki, T.; Miyamoto, Y.; Taniguchi, T.; Siyushev, P.; Metsch, M.H.; Jelezko, F.; Hatano, M. Tin-Vacancy Quantum Emitters in Diamond. *Phys. Rev. Lett.* **2017**, *119*, 253601. [CrossRef] [PubMed]
39. Ditalia Tchernij, S.; Lühmann, T.; Herzig, T.; Küpper, J.; Damin, A.; Santonocito, S.; Signorile, M.; Traina, P.; Moreva, E.; Celegato, F.; et al. Single-Photon Emitters in Lead-Implanted Single-Crystal Diamond. *ACS Photonics* **2018**, *5*, 4864–4871. [CrossRef]
40. Trusheim, M.E.; Pingault, B.; Wan, N.H.; Gündoğan, M.; De Santis, L.; Debroux, R.; Gangloff, D.; Purser, C.; Chen, K.C.; Walsh, M.; et al. Transform-Limited Photons From a Coherent Tin-Vacancy Spin in Diamond. *Phys. Rev. Lett.* **2020**, *124*, 023602. [CrossRef]

41. Görlitz, J.; Herrmann, D.; Fuchs, P.; Iwasaki, T.; Taniguchi, T.; Rogalla, D.; Hardeman, D.; Colard, P.-O.; Markham, M.; Hatano, M.; et al. Coherence of a charge tabilized tin-vacancy spin in diamond. *Npj Quantum Inf.* **2022**, *8*, 45. [CrossRef]
42. Rosenthal, E.I.; Anderson, C.P.; Kleidermacher, H.C.; Stein, A.J.; Lee, H.; Grzesik, J.; Scuri, G.; Rugar, A.E.; Riedel, D.; Aghaeimeibodi, S.; et al. Microwave Spin Control of a Tin-Vacancy Qubit in Diamond. *Phys. Rev. X* **2023**, *13*, 031022. [CrossRef]
43. Harris, I.B.; Michaels, C.P.; Chen, K.C.; Parker, R.A.; Titze, M.; Martínez, J.A.; Sutula, M.; Christen, I.R.; Stramma, A.M.; Roth, W.; et al. Hyperfine Spectroscopy of Isotopically Engineered Group-IV Color Centers in Diamond. *PRX Quantum* **2023**, *4*, 040301. [CrossRef]
44. Osmic, E.; Pezzagna, S.; Lühmann, T.; Böhlmann, W.; Meijer, J. Unusual temperature dependence of the photoluminescence emission of MgV centers in diamond. *Appl. Phys. Lett.* **2022**, *121*, 084101. [CrossRef]
45. Lühmann, T.; Diziain, S.; Meijer, J.; Pezzagna, S. Identification and Creation of the Room-Temperature Coherently Controllable ST1 Spin Center in Diamond. *ACS Photonics* **2022**, *9*, 1691–1699. [CrossRef]
46. Prestopino, G.; Marinelli, M.; Milani, E.; Verona, C.; Verona-Rinati, G.; Traina, P.; Moreva, E.; Degiovanni, I.P.; Genovese, M.; Ditalia Tchernij, S.; et al. Photo-physical properties of He-related color centers in diamond. *Appl. Phys. Lett.* **2017**, *111*, 111105. [CrossRef]
47. Sandstrom, R.; Ke, L.; Martin, A.; Wang, Z.; Kianinia, M.; Green, B.; Gao, W.-B.; Aharonovich, I. Optical properties of implanted Xe color centers in diamond. *Opt. Commun.* **2018**, *411*, 182–186. [CrossRef]
48. Ditalia Tchernij, S.; Herzig, T.; Forneris, J.; Küpper, J.; Pezzagna, S.; Traina, P.; Moreva, E.; Degiovanni, I.P.; Brida, G.; Skukan, N.; et al. Single-Photon-Emitting Optical Centers in Diamond Fabricated upon Sn Implantation. *ACS Photonics* **2017**, *4*, 2580–2586. [CrossRef]
49. Lühmann, T.; Meijer, J.; Pezzagna, S. Charge-Assisted Engineering of Color Centers in Diamond. *Phys. Status Solidi A* **2021**, *218*, 2000614. [CrossRef]
50. Wang, P.; Taniguchi, T.; Miyamoto, Y.; Hatano, M.; Iwasaki, T. Low-Temperature Spectroscopic Investigation of Lead-Vacancy Centers in Diamond Fabricated by High-Pressure and High-Temperature Treatment. *ACS Photonics* **2021**, *8*, 2947–2954. [CrossRef]
51. Chen, Y.-C.; Salter, P.S.; Knauer, S.; Weng, L.; Frangeskou, A.C.; Stephen, C.J.; Ishmael, S.N.; Dolan, P.R.; Johnson, S.; Green, B.L.; et al. Laser writing of coherent colour centres in diamond. *Nat. Photonics* **2017**, *11*, 77–80. [CrossRef]
52. Nieto Hernández, E.; Redolfi, E.; Stella, C.; Andrini, G.; Corte, E.; Sachero, S.; Ditalia Tchernij, S.; Picariello, F.; Herzig, T.; Borzdov, Y.M.; et al. Efficiency Optimization of Ge-V Quantum Emitters in Single-Crystal Diamond upon Ion Implantation and HPHT Annealing. *Adv. Quantum Technol.* **2023**, *6*, 2300010. [CrossRef]
53. Sotillo, B.; Bharadwaj, V.; Hadden, J.P.; Sakakura, M.; Chiappini, A.; Fernandez, T.T.; Longhi, S.; Jedrkiewicz, O.; Shimotsuma, Y.; Criante, L.; et al. Diamond photonics platform enabled by femtosecond laser writing. *Sci. Rep.* **2016**, *6*, 355566. [CrossRef]
54. Schröder, T.; Trusheim, M.E.; Walsh, M.; Li, L.; Zheng, J.; Schukraft, M.; Sipahigil, A.; Evans, R.E.; Sukachev, D.D.; Nguyen, C.T.; et al. Scalable focused ion beam creation of nearly lifetime-limited single quantum emitters in diamond nanostructures. *Nat. Commun.* **2017**, *8*, 15376. [CrossRef]
55. Wan, N.H.; Lu, T.-J.; Chen, K.C.; Walsh, M.P.; Trusheim, M.E.; De Santis, L.; Bersin, E.A.; Harris, I.B.; Mouradian, S.L.; Christen, I.R.; et al. Large-scale integration of artificial atoms in hybrid photonic circuits. *Nature* **2020**, *583*, 226–231. [CrossRef]
56. Balasubramanian, P.; Osterkamp, C.; Brinza, O.; Rollo, M.; Robert-Philip, I.; Goldner, P.; Jacques, V.; Jelezko, F.; Achard, J.; Tallaire, A. Enhancement of the creation yield of NV ensembles in a chemically vapour deposited diamond. *Carbon* **2022**, *194*, 282–289. [CrossRef]
57. Ekimov, E.; Lyapin, S.; Kondrin, M. Tin-vacancy color centers in micro- and polycrystalline diamonds synthesized at high pressures. *Diam. Relat. Mater.* **2018**, *87*, 223–227. [CrossRef]
58. Palyanov, Y.N.; Kupriyanov, I.N.; Borzdov, Y.M. High-pressure synthesis and characterization of Sn-doped single crystal diamond. *Carbon* **2019**, *143*, 769–775. [CrossRef]
59. Engel, J.; Jhuria, K.; Polley, D.; Lühmann, T.; Kuhrke, M.; Liu, W.; Bokor, J.; Schenkel, T.; Wunderlich, R. Combining femtosecond laser annealing and shallow ion implantation for local color center creation in diamond. *Appl. Phys. Lett.* **2023**, *122*, 234002. [CrossRef]
60. Wang, X.; Fang, H.; Sun, F.; Sun, H. Laser Writing of Color Centers. *Laser Photonics Rev.* **2022**, *16*, 2100029. [CrossRef]
61. Schukraft, M.; Zheng, J.; Schröder, T.; Mouradian, S.L.; Walsh, M.; Trusheim, M.E.; Bakhru, H.; Englund, D.R. Invited Article: Precision nanoimplantation of nitrogen vacancy centers into diamond photonic crystal cavities and waveguides. *APL Photonics* **2016**, *1*, 020801. [CrossRef]
62. Evans, R.E.; Bhaskar, M.K.; Sukachev, D.D.; Nguyen, C.T.; Si pahigil, A.; Burek, M.J.; Machielse, B.; Zhang, G.H.; Zibrov, A.S.; Bielejec, E.; et al. Photon-mediated interactions between quantum emitters in a diamond nanocavity. *Science* **2018**, *362*, 662–665. [CrossRef]
63. Burek, M.J.; Meuwly, C.; Evans, R.E.; Bhaskar, M.K.; Sipahigil, A.; Meesala, S.; Machielse, B.; Sukachev, D.D.; Nguyen, C.T.; Pacheco, J.L.; et al. Fiber-Coupled Diamond Quantum Nanophotonic Interface. *Phys. Rev. Appl.* **2017**, *8*, 024026. [CrossRef]
64. Koch, M.K.; Hoese, M.; Bharadwaj, V.; Lang, J.; Hadden, J.P.; Ramponi, R.; Jelezko, F.; Eaton, S.M.; Kubanek, A. Super-Poissonian Light Statistics from Individual Silicon Vacancy Centers Coupled to a Laser-Written Diamond Waveguide. *ACS Photonics* **2022**, *9*, 3366–3373. [CrossRef]

65. Hausmann, B.J.M.; Shields, B.; Quan, Q.; Maletinsky, P.; McCutcheon, M.; Choy, J.T.; Babinec, T.M.; Kubanek, A.; Yacoby, A.; Lukin, M.D.; et al. Integrated Diamond Networks for Quantum Nanophotonics. *Nano Lett.* **2012**, *12*, 1578–1582. [CrossRef] [PubMed]
66. Sipahigil, A.; Evans, R.E.; Sukachev, D.D.; Burek, M.J.; Borregaard, J.; Bhaskar, M.K.; Nguyen, C.T.; Pacheco, J.L.; Atikian, H.A.; Meuwly, C.; et al. An integrated diamond nanophotonics platform for quantum-optical networks. *Science* **2016**, *354*, 847–850. [CrossRef]
67. Rugar, A.E.; Aghaeimeibodi, S.; Riedel, D.; Dory, C.; Lu, H.; McQuade, P.J.; Shen, Z.-X.; Melosh, N.A.; Vučković, J. Quantum Photonic Interface for Tin-Vacancy Centers in Diamond. *Phys. Rev. X* **2021**, *11*, 031021. [CrossRef]
68. Fuchs, P.; Jung, T.; Kieschnick, M.; Meijer, J.; Becher, C. A cavity-based optical antenna for color centers in diamond. *APL Photonics* **2021**, *6*, 086102. [CrossRef]
69. Lohrmann, A.; Pezzagna, S.; Dobrinets, I.; Spinicelli, P.; Jacques, V.; Roch, J.-F.; Meijer, J.; Zaitsev, A.M. Diamond based light-emitting diode for visible single-photon emission at room temperature. *Appl. Phys. Lett.* **2011**, *99*, 251106. [CrossRef]
70. Mizuochi, N.; Makino, T.; Kato, H.; Takeuchi, D.; Ogura, M.; Okushi, H.; Nothaft, M.; Neumann, P.; Gali, A.; Jelezko, F.; et al. Electrically driven single-photon source at room temperature in diamond. *Nat. Photonics* **2012**, *6*, 299–303. [CrossRef]
71. Bray, K.; Fedyanin, D.Y.; Khramtsov, I.A.; Bilokur, M.O.; Regan, B.; Toth, M.; Aharonovich, I. Electrical excitation and charge-state conversion of silicon vacancy color centers in single-crystal diamond membranes. *Appl. Phys. Lett.* **2020**, *116*, 101103. [CrossRef]
72. Eddy, C.R.; Gaskill, D.K. Silicon Carbide as a Platform for Power Electronics. *Science* **2009**, *324*, 1398–1400. [CrossRef]
73. Masri, P. Silicon carbide and silicon carbide-based structures: The physics of epitaxy. *Surf. Sci. Rep.* **2002**, *48*, 1–51. [CrossRef]
74. Castelletto, S.; Boretti, A. Silicon carbide color centers for quantum applications. *J. Phys. Photonics* **2020**, *2*, 022001. [CrossRef]
75. Sörman, E.; Son, N.T.; Chen, W.M.; Kordina, O.; Hallin, C.; Janzen, E. Silicon vacancy related defect in 4H and 6H SiC. *Phys. Rev. B* **2000**, *61*, 2613–2620. [CrossRef]
76. Baranov, P.G.; Bundakova, A.P.; Soltamova, A.A.; Orlinskii, S.B.; Borovykh, I.V.; Zondervan, R.; Verberk, R.; Schmidt, J. Silicon vacancy in SiC as a promising quantum system for single-defect and single-photon spectroscopy. *Phys. Rev. B* **2011**, *83*, 125203. [CrossRef]
77. Widmann, M.; Lee, S.-Y.; Rendler, T.; Son, N.T.; Fedder, H.; Paik, S.; Yang, L.-P.; Zhao, N.; Yang, S.; Booker, I.; et al. Coherent control of single spins in silicon carbide at room temperature. *Nat. Mater.* **2015**, *14*, 164–168. [CrossRef]
78. Nagy, R.; Niethammer, M.; Widmann, M.; Chen, Y.-C.; Udvarhelyi, P.; Bonato, C.; Hassan, J.U.; Karhu, R.; Ivanov, I.G.; Son, N.T.; et al. High-fidelity spin and optical control of single silicon-vacancy centres in silicon carbide. *Nat. Commun.* **2019**, *10*, 1954. [CrossRef]
79. Fischer, M.; Sperlich, A.; Kraus, H.; Ohshima, T.; Astakhov, G.V.; Dyakonov, V. Highly Efficient Optical Pumping of Spin Defects in Silicon Carbide for Stimulated Microwave Emission. *Phys. Rev. Appl.* **2018**, *9*, 054006. [CrossRef]
80. Lee, S.-Y.; Niethammer, M.; Wrachtrup, J. Vector magnetometry based on S=3/2 electronic spins. *Phys. Rev. B* **2015**, *92*, 115201. [CrossRef]
81. Abraham, J.B.S.; Gutgsell, C.; Todorovski, D.; Sperling, S.; Epstein, J.E.; Tien-Street, B.S.; Sweeney, T.M.; Wathen, J.J.; Pogue, E.A.; Brereton, P.G.; et al. Nanotesla Magnetometry with the Silicon Vacancy in Silicon Carbide. *Phys. Rev. Appl.* **2021**, *15*, 064022. [CrossRef]
82. Kraus, H.; Soltamov, V.A.; Fuchs, F.; Simin, D.; Sperlich, A.; Baranov, P.G.; Astakhov, G.V.; Dyakonov, V. Magnetic field and temperature sensing with atomic-scale spin defects in silicon carbide. *Sci. Rep.* **2015**, *4*, 5303. [CrossRef]
83. Lohrmann, A.; Iwamoto, N.; Bodrog, Z.; Castelletto, S.; Ohshima, T.; Karle, T.; Gali, A.; Prawer, S.; McCallum, J.; Johnson, B. Single-photon emitting diode in silicon carbide. *Nat. Commun.* **2015**, *6*, 7783. [CrossRef]
84. Lohrmann, A.; Johnson, B.C.; McCallum, J.C.; Castelletto, S. A review on single photon sources in silicon carbide. *Rep. Prog. Phys.* **2017**, *80*, 034502. [CrossRef]
85. Umeda, T.; Ishoya, J.; Ohshima, T.; Morishita, N.; Itoh, H.; Gali, A. Identification of positively charged carbon antisite-vacancy pairs in4H−SiC. *Phys. Rev. B* **2007**, *75*, 245202. [CrossRef]
86. Castelletto, S.; Johnson, B.C.; Ivády, V.; Stavrias, N.; Umeda, T.; Gali, A.; Ohshima, T. A silicon carbide room-temperature single-photon source. *Nat. Mater.* **2014**, *13*, 151–156. [CrossRef]
87. Wang, J.; Zhang, X.; Zhou, Y.; Li, K.; Wang, Z.; Peddibhotla, P.; Liu, F.; Bauerdick, S.; Rudzinski, A.; Liu, Z.; et al. Scalable Fabrication of Single Silicon Vacancy Defect Arrays in Silicon Carbide Using Focused Ion Beam. *ACS Photonics* **2017**, *4*, 1054–1059. [CrossRef]
88. Ohshima, T.; Satoh, T.; Kraus, H.; Astakhov, G.V.; Dyakonov, V.V.; Baranov, P.G. Creation of silicon vacancy in silicon carbide by proton beam writing toward quantum sensing applications. *J. Phys. D Appl. Phys.* **2018**, *51*, 333002. [CrossRef]
89. Yan, F.-F.; Yi, A.-L.; Wang, J.-F.; Li, Q.; Yu, P.; Zhang, J.-X.; Gali, A.; Wang, Y.; Xu, J.-S.; Ou, X.; et al. Room-temperature coherent control of implanted defect spins in silicon carbide. *Npj Quantum Inf.* **2020**, *6*, 38. [CrossRef]
90. Radulaski, M.; Widmann, M.; Niethammer, M.; Zhang, J.L.; Lee, S.-Y.; Rendler, T.; Lagoudakis, K.G.; Son, N.T.; Janzén, E.; Ohshima, T.; et al. Scalable Quantum Photonics with Single Color Centers in Silicon Carbide. *Nano Lett.* **2017**, *17*, 1782–1786. [CrossRef]
91. Fuchs, F.; Soltamov, V.A.; Väth, S.; Baranov, P.G.; Mokhov, E.N.; Astakhov, G.V.; Dyakonov, V. Silicon carbide light-emitting diode as a prospective room temperature source for single photons. *Sci. Rep.* **2013**, *3*, 1637. [CrossRef]

92. Chen, Y.-C.; Salter, P.S.; Niethammer, M.; Widmann, M.; Kaiser, F.; Nagy, R.; Morioka, N.; Babin, C.; Erlekampf, J.; Berwian, P.; et al. Laser Writing of Scalable Single Color Centers in Silicon Carbide. *Nano Lett.* **2019**, *19*, 2377–2383. [CrossRef]
93. Wang, J.-F.; Yan, F.-F.; Li, Q.; Liu, Z.-H.; Liu, H.; Guo, G.-P.; Guo, L.-P.; Zhou, X.; Cui, J.-M.; Wang, J.; et al. Coherent Control of Nitrogen-Vacancy Center Spins in Silicon Carbide at Room Temperature. *Phys. Rev. Lett.* **2020**, *124*, 223601. [CrossRef]
94. Sato, S.-I.; Narahara, T.; Abe, Y.; Hijikata, Y.; Umeda, T.; Ohshima, T. Formation of nitrogen-vacancy centers in 4H-SiC and their near infrared photoluminescence properties. *J. Appl. Phys.* **2019**, *126*, 083105. [CrossRef]
95. Wolfowicz, G.; Anderson, C.P.; Diler, B.; Poluektov, O.G.; Heremans, F.J.; Awschalom, D.D. Vanadium spin qubits as telecom quantum emitters in silicon carbide. *Sci. Adv.* **2020**, *6*, eaaz1192. [CrossRef]
96. Ou, H.; Shi, X.; Lu, Y.; Kollmuss, M.; Steiner, J.; Tabouret, V.; Syväjärvi, M.; Wellmann, P.; Chaussende, D. Novel Photonic Applications of Silicon Carbide. *Materials* **2023**, *16*, 1014. [CrossRef]
97. Sardi, F.; Kornher, T.; Widmann, M.; Kolesov, R.; Schiller, F.; Reindl, T.; Hagel, M.; Wrachtrup, J. Scalable production of solid-immersion lenses for quantum emitters in silicon carbide. *Appl. Phys. Lett.* **2020**, *117*, 022105. [CrossRef]
98. Crook, A.L.; Anderson, C.P.; Miao, K.C.; Bourassa, A.; Lee, H.; Bayliss, S.L.; Bracher, D.O.; Zhang, X.; Abe, H.; Ohshima, T.; et al. Purcell Enhancement of a Single Silicon Carbide Color Center with Coherent Spin Control. *Nano Lett.* **2020**, *20*, 3427–3434. [CrossRef]
99. Bracher, D.O.; Zhang, X.; Hu, E.L. Selective Purcell enhancement of two closely linked zero-phonon transitions of a silicon carbide color center. *Proc. Natl. Acad. Sci. USA* **2017**, *114*, 4060–4065. [CrossRef]
100. Lukin, D.M.; Dory, C.; Guidry, M.A.; Yang, K.Y.; Mishra, S.D.; Trivedi, R.; Radulaski, M.; Sun, S.; Vercruysse, D.; Ahn, G.H.; et al. 4H-silicon-carbide-on-insulator for integrated quantum and nonlinear photonics. *Nat. Photonics* **2020**, *14*, 330–334. [CrossRef]
101. Davies, G. The optical properties of luminescence centres in silicon. *Phys. Rep.* **1989**, *176*, 83–188. [CrossRef]
102. Safonov, A.N.; Lightowlers, E.C.; Davies, G.; Leary, P.; Jones, R.; Öberg, S. Interstitial-Carbon Hydrogen Interaction in Silicon. *Phys. Rev. Lett.* **1996**, *77*, 4812–4815. [CrossRef]
103. Beaufils, C.; Redjem, W.; Rousseau, E.; Jacques, V.; Kuznetsov, A.Y.; Raynaud, C.; Voisin, C.; Benali, A.; Herzig, T.; Pezzagna, S.; et al. Optical properties of an ensemble of G-centers in silicon. *Phys. Rev. B* **2018**, *97*, 035303. [CrossRef]
104. Rotem, E.; Shainline, J.M.; Xu, J.M. Electroluminescence of nanopatterned silicon with carbon implantation and solid phase epitaxial regrowth. *Opt. Express* **2007**, *15*, 14099–14106. [CrossRef]
105. Murata, K.; Yasutake, Y.; Nittoh, K.-I.; Fukatsu, S.; Miki, K. High-density G-centers, light-emitting point defects in silicon crystal. *AIP Adv.* **2011**, *1*, 032125. [CrossRef]
106. Redjem, W.; Durand, A.; Herzig, T.; Benali, A.; Pezzagna, S.; Meijer, J.; Kuznetsov, A.Y.; Nguyen, H.S.; Cueff, S.; Gérard, J.-M.; et al. Single artificial atoms in silicon emitting at telecom wavelengths. *Nat. Electron.* **2020**, *3*, 738–743. [CrossRef]
107. Hollenbach, M.; Berencén, Y.; Kentsch, U.; Helm, M.; Astakhov, G.V. Engineering telecom single-photon emitters in silicon for scalable quantum photonics. *Opt. Express* **2020**, *28*, 26111–26121. [CrossRef]
108. Udvarhelyi, P.; Somogyi, B.; Thiering, G.; Gali, A. Identification of a Telecom Wavelength Single Photon Emitter in Silicon. *Phys. Rev. Lett.* **2021**, *127*, 196402. [CrossRef]
109. Chartrand, C.; Bergeron, L.; Morse, K.J.; Riemann, H.; Abrosimov, N.V.; Becker, P.; Pohl, H.-J.; Simmons, S.; Thewalt, M.L.W. Highly enriched Si28 reveals remarkable optical linewidths and fine structure for well-known damage centers. *Phys. Rev. B* **2018**, *98*, 195201. [CrossRef]
110. Lee, K.M.; O'Donnell, K.P.; Weber, J.; Cavenett, B.C.; Watkins, G.D. Optical Detection of Magnetic Resonance for a Deep-Level Defect in Silicon. *Phys. Rev. Lett.* **1982**, *48*, 37–40. [CrossRef]
111. Buckley, S.M.; Tait, A.N.; Moody, G.; Primavera, B.; Olson, S.; Herman, J.; Silverman, K.L.; Rao, S.P.; Nam, S.W.; Mirin, R.P.; et al. Optimization of photoluminescence from W centers in silicon-on-insulator. *Opt. Express* **2020**, *28*, 16057–16072. [CrossRef]
112. Udvarhelyi, P.; Pershin, A.; Deák, P.; Gali, A. An L-band emitter with quantum memory in silicon. *Npj Comput. Mater.* **2022**, *8*, 262. [CrossRef]
113. MacQuarrie, E.; Chartrand, C.; Higginbottom, D.; Morse, K.; A Karasyuk, V.; Roorda, S.; Simmons, S. Generating T centres in photonic silicon-on-insulator material by ion implantation. *New J. Phys.* **2021**, *23*, 103008. [CrossRef]
114. Dhaliah, D.; Xiong, Y.; Sipahigil, A.; Griffin, S.M.; Hautier, G. First-principles study of the T center in silicon. *Phys. Rev. Mater.* **2022**, *6*, L053201. [CrossRef]
115. Higginbottom, D.B.; Kurkjian, A.T.K.; Chartrand, C.; Kazemi, M.; Brunelle, N.A.; MacQuarrie, E.R.; Klein, J.R.; Lee-Hone, N.R.; Stacho, J.; Ruether, M.; et al. Optical observation of single spins in silicon. *Nature* **2022**, *607*, 266–270. [CrossRef]
116. Bergeron, L.; Chartrand, C.; Kurkjian, A.T.K.; Morse, K.J.; Riemann, H.; Abrosimov, N.V.; Becker, P.; Pohl, H.-J.; Thewalt, M.L.W.; Simmons, S. Silicon-Integrated Telecommunications Photon-Spin Interface. *PRX Quantum* **2020**, *1*, 020301. [CrossRef]
117. Baron, Y.; Durand, A.; Udvarhelyi, P.; Herzig, T.; Khoury, M.; Pezzagna, S.; Meijer, J.; Robert-Philip, I.; Abbarchi, M.; Hartmann, J.-M.; et al. Detection of Single W-Centers in Silicon. *ACS Photonics* **2022**, *9*, 2337–2345. [CrossRef]
118. Davies, G.; Lightowlers, E.C.; Ciechanowska, Z.E. The 1018 meV (W or I_1) vibronic band in silicon. *J. Phys. C Solid State Phys.* **1987**, *20*, 191–205. [CrossRef]
119. Giri, P.K. Photoluminescence signature of silicon interstitial cluster evolution from compact to extended structures in ion-implanted silicon. *Semicond. Sci. Technol.* **2005**, *20*, 638–644. [CrossRef]
120. Nakamura, M.; Nagai, S. Influence of high-energy electron irradiation on the formation and annihilation of the photoluminescence *W* center and the center's origin in a proton-implanted silicon crystal. *Phys. Rev. B* **2002**, *66*, 155204. [CrossRef]

121. Kirkpatrick, C.G.; Noonan, J.R.; Streetman, B.G. Recombination luminescence from ion implanted silicon. *Radiat. Eff.* **1976**, *30*, 97–106. [CrossRef]
122. Davies, G.; Oates, A.S.; Newman, R.C.; Woolley, R.; Lightowlers, E.C.; Binns, M.J.; Wilkes, J.G. Carbon-related radiation damage centres in Czochralski silicon. *J. Phys. C: Solid State Phys.* **1986**, *19*, 841–855. [CrossRef]
123. Kürner, W.; Sauer, R.; Dörnen, A.; Thonke, K. Structure of the 0.767-eV oxygen-carbon luminescence defect in 450 °C thermally annealed Czochralski-grown silicon. *Phys. Rev. B* **1989**, *39*, 13327–13337. [CrossRef]
124. Bean, A.; Newman, R.; Smith, R. Electron irradiation damage in silicon containing carbon and oxygen. *J. Phys. Chem. Solids* **1970**, *31*, 739–751. [CrossRef]
125. Ishikawa, T.; Koga, K.; Itahashi, T.; Itoh, K.M.; Vlasenko, L.S. Optical properties of triplet states of excitons bound to interstitial-carbon interstitial-oxygen defects in silicon. *Phys. Rev. B* **2011**, *84*, 115204. [CrossRef]
126. Durand, A.; Baron, Y.; Redjem, W.; Herzig, T.; Benali, A.; Pezzagna, S.; Meijer, J.; Kuznetsov, A.Y.; Gérard, J.-M.; Robert-Philip, I.; et al. Broad Diversity of Near-Infrared Single-Photon Emitters in Silicon. *Phys. Rev. Lett.* **2021**, *126*, 083602. [CrossRef]
127. Baron, Y.; Durand, A.; Herzig, T.; Khoury, M.; Pezzagna, S.; Meijer, J.; Robert-Philip, I.; Abbarchi, M.; Hartmann, J.-M.; Reboh, S.; et al. Single G centers in silicon fabricated by co-implantation with carbon and proton. *Appl. Phys. Lett.* **2022**, *121*, 084003. [CrossRef]
128. Hollenbach, M.; Klingner, N.; Jagtap, N.S.; Bischoff, L.; Fowley, C.; Kentsch, U.; Hlawacek, G.; Erbe, A.; Abrosimov, N.V.; Helm, M.; et al. Wafer-scale nanofabrication of telecom single-photon emitters in silicon. *Nat. Commun.* **2022**, *13*, 7683. [CrossRef] [PubMed]
129. Zhiyenbayev, Y.; Redjem, W.; Ivanov, V.; Qarony, W.; Papapanos, C.; Simoni, J.; Liu, W.; Jhuria, K.; Tan, L.Z.; Schenkel, T.; et al. Scalable manufacturing of quantum light emitters in silicon under rapid thermal annealing. *Opt. Express* **2023**, *31*, 8352–8362. [CrossRef] [PubMed]
130. Liu, W.; Ivanov, V.; Jhuria, K.; Ji, Q.; Persaud, A.; Redjem, W.; Simoni, J.; Zhiyenbayev, Y.; Kante, B.; Lopez, J.G.; et al. Quantum Emitter Formation Dynamics and Probing of Radiation-Induced Atomic Disorder in Silicon. *Phys. Rev. Appl.* **2023**, *20*, 014058. [CrossRef]
131. Davies, G.; Kun, K.T.; Reade, T. Annealing kinetics of the dicarbon radiation-damage center in crystalline silicon. *Phys. Rev. B* **1991**, *44*, 12146–12157. [CrossRef] [PubMed]
132. Andrini, G.; Zanelli, G.; Ditalia Tchernij, S.; Corte, E.; Hernandez, E.N.; Verna, A.; Cocuzza, M.; Bernardi, E.; Virzi, S.; Traina, P.; et al. Study of W centers formation in silicon upon ion implantation and rapid thermal annealing. In Proceedings of the 2023 IEEE Photonics Society Summer Topicals Meeting Series (SUM), Sicily, Italy, 17–19 July 2023. [CrossRef]
133. Redjem, W.; Amsellem, A.J.; Allen, F.I.; Benndorf, G.; Bin, J.; Bulanov, S.; Esarey, E.; Feldman, L.C.; Fernandez, J.F.; Lopez, J.G.; et al. Defect engineering of silicon with ion pulses from laser acceleration. *Commun. Mater.* **2023**, *4*, 22. [CrossRef]
134. Andrini, G.; Zanelli, G.; Ditalia Tchernij, S.; Corte, E.; Hernandez, E.N.; Verna, A.; Cocuzza, M.; Bernardi, E.; Virzì, S.; Traina, P.; et al. Efficient activation of telecom emitters in silicon upon ns pulsed laser annealing. *arXiv* **2023**, arXiv:2304.10132.
135. Quard, H.; Khoury, M.; Wang, A.; Herzig, T.; Meijer, J.; Pezzagna, S.; Wood, T. Femtosecond laser induced creation of G and W-centers in silicon-on-insulator substrates. *arXiv* **2023**, arXiv:2304.03551.
136. Skolnick, M.S.; Cullis, A.G.; Webber, H. Defect photoluminescence from pulsed-laser-annealed ion-implanted Si. *Appl. Phys. Lett.* **1981**, *38*, 464–466. [CrossRef]
137. Skolnick; Cullis, A.G.; Webber, H. Defect photoluminescence from Si laser annealed over a wide temperature range. *J. Lumin.* **1981**, *24–25*, 39–42. [CrossRef]
138. Ristori, A.; Khoury, M.; Salvalaglio, M.; Filippatos, A.; Amato, M.; Herzig, T.; Meijer, J.; Pezzagna, S.; Hannani, D.; Bollani, M.; et al. Strain Engineering of the Electronic States of Silicon-Based Quantum Emitters. *Adv. Opt. Mater.* **2023**, *12*, 2301608. [CrossRef]
139. Hollenbach, M.; Jagtap, N.S.; Fowley, C.; Baratech, J.; Guardia-Arce, V.; Kentsch, U.; Eichler-Volf, A.; Abrosimov, N.V.; Erbe, A.; Shin, C.; et al. Metal-assisted chemically etched silicon nanopillars hosting telecom photon emitters. *J. Appl. Phys.* **2022**, *132*, 033101. [CrossRef]
140. Buckley, S.; Chiles, J.; McCaughan, A.N.; Moody, G.; Silverman, K.L.; Stevens, M.J.; Mirin, R.P.; Nam, S.W.; Shainline, J.M. All-silicon light-emitting diodes waveguide-integrated with superconducting single-photon detectors. *Appl. Phys. Lett.* **2017**, *111*, 141101. [CrossRef]
141. Tait, A.; Buckley, S.; Chiles, J.; McCaughan, A.N.; Olson, S.; Rao, S.P.; Nam, S.W.; Mirin, R.; Shainline, J. Microring resonator-coupled photoluminescence from silicon W centers. *J. Phys. Photonics* **2020**, *2*, 045001. [CrossRef]
142. Prabhu, M.; Errando-Herranz, C.; De Santis, L.; Christen, I.; Chen, C.; Gerlach, C.; Englund, D. Individually addressable and spectrally programmable artificial atoms in silicon photonics. *Nat. Commun.* **2023**, *14*, 2380. [CrossRef]
143. Vyas, K.; Espinosa, D.H.G.; Hutama, D.; Jain, S.K.; Mahjoub, R.; Mobini, E.; Awan, K.M.; Lundeen, J.; Dolgaleva, K. Group III-V semiconductors as promising nonlinear integrated photonic platforms. *Adv. Phys. X* **2022**, *7*, 2097020. [CrossRef]
144. Parto, K.; Azzam, S.I.; Lewis, N.; Patel, S.D.; Umezawa, S.; Watanabe, K.; Taniguchi, T.; Moody, G. Cavity-Enhanced 2D Material Quantum Emitters Deterministically Integrated with Silicon Nitride Microresonators. *Nano Lett.* **2022**, *22*, 9748–9756. [CrossRef] [PubMed]
145. Hersee, S.D.; Sun, X.; Wang, X. The Controlled Growth of GaN Nanowires. *Nano Lett.* **2006**, *6*, 1808–1811. [CrossRef] [PubMed]

146. Mnaymneh, K.; Dalacu, D.; McKee, J.; Lapointe, J.; Haffouz, S.; Weber, J.F.; Northeast, D.B.; Poole, P.J.; Aers, G.C.; Williams, R.L. On-Chip Integration of Single Photon Sources via Evanescent Coupling of Tapered Nanowires to SiN Waveguides. *Adv. Quantum Technol.* **2019**, *3*, 201900021. [CrossRef]
147. Wang, X.-D.; Zhu, Y.-F.; Jin, T.-T.; Ou, W.-W.; Ou, X.; Zhang, J.-X. Waveguide-coupled deterministic quantum light sources and post-growth engineering methods for integrated quantum photonics. *Chip* **2022**, *1*, 100018. [CrossRef]
148. Rajbhandari, S.; McKendry, J.J.; Herrnsdorf, J.; Chun, H.; Faulkner, G.; Haas, H.; Watson, I.M.; O'Brien, D.; Dawson, M.D. A review of gallium nitride LEDs for multi-gigabit-per-second visible light data communications. *Semicond. Sci. Technol.* **2017**, *32*, 023001. [CrossRef]
149. Li, X.; Wang, Y.; Hane, K.; Shi, Z.; Yan, J. GaN-based integrated photonics chip with suspended LED and waveguide. *Opt. Commun.* **2018**, *415*, 43–47. [CrossRef]
150. Gromovyi, M.; El Kurdi, M.; Checoury, X.; Herth, E.; Tabataba-Vakili, F.; Bhat, N.; Courville, A.; Semond, F.; Boucaud, P. Low-loss GaN-on-insulator platform for integrated photonics. *Opt. Express* **2022**, *30*, 20737–20749. [CrossRef]
151. Zhang, Y.; McKnight, L.; Engin, E.; Watson, I.M.; Cryan, M.J.; Gu, E.; Thompson, M.G.; Calvez, S.; O'brien, J.L.; Dawson, M.D. GaN directional couplers for integrated quantum photonics. *Appl. Phys. Lett.* **2011**, *99*, 161119. [CrossRef]
152. Berhane, A.M.; Jeong, K.; Bodrog, Z.; Fiedler, S.; Schröder, T.; Triviño, N.V.; Palacios, T.; Gali, A.; Toth, M.; Englund, D.; et al. Bright Room-Temperature Single-Photon Emission from Defects in Gallium Nitride. *Adv. Mater.* **2017**, *29*, 12. [CrossRef]
153. Berhane, A.M.; Jeong, K.-Y.; Bradac, C.; Walsh, M.; Englund, D.; Toth, M.; Aharonovich, I. Photophysics of GaN single-photon emitters in the visible spectral range. *Phys. Rev. B* **2018**, *97*, 165202. [CrossRef]
154. Nguyen, M.; Zhu, T.; Kianinia, M.; Massabuau, F.; Aharonovich, I.; Toth, M.; Oliver, R.; Bradac, C. Effects of microstructure and growth conditions on quantum emitters in gallium nitride. *APL Mater.* **2019**, *7*, 081106. [CrossRef]
155. Bishop, S.G.; Hadden, J.P.; Hekmati, R.; Cannon, J.K.; Langbein, W.W.; Bennett, A.J. Enhanced light collection from a gallium nitride color center using a near index-matched solid immersion lens. *Appl. Phys. Lett.* **2022**, *120*, 114001. [CrossRef]
156. Nguyen, M.A.P.; Hite, J.; Mastro, M.A.; Kianinia, M.; Toth, M.; Aharonovich, I. Site control of quantum emitters in gallium nitride by polarity. *Appl. Phys. Lett.* **2021**, *118*, 021103. [CrossRef]
157. Zhou, Y.; Wang, Z.; Rasmita, A.; Kim, S.; Berhane, A.; Bodrog, Z.; Adamo, G.; Gali, A.; Aharonovich, I.; Gao, W.-B. Room temperature solid-state quantum emitters in the telecom range. *Sci. Adv.* **2018**, *4*, eaar3580. [CrossRef]
158. Meunier, M.; Eng, J.J.H.; Mu, Z.; Chenot, S.; Brändli, V.; de Mierry, P.; Gao, W.; Zúñiga-Pérez, J. Telecom single-photon emitters in GaN operating at room temperature: Embedment into bullseye antennas. *Nanophotonics* **2023**, *12*, 1405–1419. [CrossRef]
159. Xiong, C.; Pernice, W.H.P.; Sun, X.; Schuck, C.; Fong, K.Y.; Tang, H.X. Aluminum nitride as a new material for chip-scale optomechanics and nonlinear optics. *New J. Phys.* **2012**, *14*, 095014. [CrossRef]
160. Xue, Y.; Chen, F.; Fang, Z.; Zhang, S.; Li, Q.; Li, M.; Kang, J.; Zhang, J.; Shen, S.; Wu, B.; et al. Bright room temperature near-infrared single-photon emission from single point defects in the AlGaN film. *Appl. Phys. Lett.* **2021**, *118*, 131103. [CrossRef]
161. Xue, Y.; Wang, H.; Xie, N.; Yang, Q.; Xu, F.; Shen, B.; Shi, J.-J.; Jiang, D.; Dou, X.; Yu, T.; et al. Single-Photon Emission from Point Defects in Aluminum Nitride Films. *J. Phys. Chem. Lett.* **2020**, *11*, 2689–2694. [CrossRef]
162. Bishop, S.G.; Hadden, J.P.; Alzahrani, F.D.; Hekmati, R.; Huffaker, D.L.; Langbein, W.W.; Bennett, A.J. Room-Temperature Quantum Emitter in Aluminum Nitride. *ACS Photonics* **2020**, *7*, 1636–1641. [CrossRef]
163. Nieto Hernández, E.; Yağcı, H.B.; Pugliese, V.; Aprà, P.; Cannon, J.K.; Bishop, S.G.; Forneris, J. Fabrication of quantum emitters in aluminium nitride by Al-ion implantation and thermal annealing. *arXiv* **2023**, arXiv:2310.20540.
164. Wang, X.J.; Zhao, S.; Fang, H.H.; Xing, R.; Chai, Y.; Li, X.Z.; Sun, H.B. Quantum Emitters with Narrow Band and High Debye–Waller Factor in Aluminum Nitride Written by Femtosecond Laser. *Nano Lett.* **2023**, *23*, 2743. [CrossRef]
165. Tu, Y.; Tang, Z.; Zhao, X.G.; Chen, Y.; Zhu, Z.Q.; Chu, J.H.; Fang, J.C. A paramagnetic neutral VAlON center in wurtzite AlN for spin qubit application. *Appl. Phys. Lett.* **2013**, *103*, 072103. [CrossRef]
166. Liu, X.; Bruch, A.W.; Gong, Z.; Lu, J.; Surya, J.B.; Zhang, L.; Wang, J.; Yan, J.; Tang, H.X. Ultra-high-Q UV microring resonators based on a single-crystalline AlN platform. *Optica* **2018**, *5*, 1279–1282. [CrossRef]
167. Li, N.; Ho, C.P.; Zhu, S.; Fu, Y.H.; Zhu, Y.; Lee, L.Y.T. Aluminium nitride integrated photonics: A review. *Nanophotonics* **2021**, *10*, 2347–2387. [CrossRef]
168. Lu, T.-J.; Lienhard, B.; Jeong, K.-Y.; Moon, H.; Iranmanesh, A.; Grosso, G.; Englund, D.R. Bright High-Purity Quantum Emitters in Aluminum Nitride Integrated Photonics. *ACS Photonics* **2020**, *7*, 2650–2657. [CrossRef]
169. Tran, T.T.; Elbadawi, C.; Totonjian, D.; Lobo, C.J.; Grosso, G.; Moon, H.; Englund, D.R.; Ford, M.J.; Aharonovich, I.; Toth, M. Robust Multicolor Single Photon Emission from Point Defects in Hexagonal Boron Nitride. *ACS Nano* **2016**, *10*, 7331–7338. [CrossRef] [PubMed]
170. Senichev, A.; Peana, S.; Martin, Z.O.; Yesilyurt, O.; Sychev, D.; Lagutchev, A.S.; Boltasseva, A.; Shalaev, V.M. Silicon Nitride Waveguides with Intrinsic Single-Photon Emitters for Integrated Quantum Photonics. *ACS Photonics* **2022**, *9*, 3357–3365. [CrossRef]
171. Tran, T.T.; Bray, K.; Ford, M.J.; Toth, M.; Aharonovich, I. Quantum emission from hexagonal boron nitride monolayers. *Nat. Nanotechnol.* **2016**, *11*, 37–41. [CrossRef]
172. Abdi, M.; Chou, J.-P.; Gali, A.; Plenio, M.B. Color Centers in Hexagonal Boron Nitride Monolayers: A Group Theory and Ab Initio Analysis. *ACS Photonics* **2018**, *5*, 1967–1976. [CrossRef]
173. Castelletto, S.; A Inam, F.; Sato, S.-I.; Boretti, A. Hexagonal boron nitride: A review of the emerging material platform for single-photon sources and the spin–photon interface. *Beilstein J. Nanotechnol.* **2020**, *11*, 740–769. [CrossRef]

174. Hayee, F.; Yu, L.; Zhang, J.L.; Ciccarino, C.J.; Nguyen, M.; Marshall, A.F.; Aharonovich, I.; Vučković, J.; Narang, P.; Heinz, T.F.; et al. Revealing multiple classes of stable quantum emitters in hexagonal boron nitride with correlated optical and electron microscopy. *Nat. Mater.* **2020**, *19*, 534–539. [CrossRef]
175. Gottscholl, A.; Kianinia, M.; Soltamov, V.; Orlinskii, S.; Mamin, G.; Bradac, C.; Kasper, C.; Krambrock, K.; Sperlich, A.; Toth, M.; et al. Initialization and read-out of intrinsic spin defects in a van der Waals crystal at room temperature. *Nat. Mater.* **2020**, *19*, 540–545. [CrossRef]
176. Mendelson, N.; Chugh, D.; Reimers, J.R.; Cheng, T.S.; Gottscholl, A.; Long, H.; Mellor, C.J.; Zettl, A.; Dyakonov, V.; Beton, P.H.; et al. Identifying carbon as the source of visible single-photon emission from hexagonal boron nitride. *Nat. Mater.* **2021**, *20*, 321–328. [CrossRef]
177. Gale, A.; Scognamiglio, D.; Zhigulin, I.; Whitefield, B.; Kianinia, M.; Aharonovich, I.; Toth, M. Manipulating the Charge State of Spin Defects in Hexagonal Boron Nitride. *Nano Lett.* **2023**, *23*, 6141–6147. [CrossRef] [PubMed]
178. Haykal, A.; Tanos, R.; Minotto, N.; Durand, A.; Fabre, F.; Li, J.; Edgar, J.H.; Ivády, V.; Gali, A.; Michel, T.; et al. Decoherence of V spin defects in monoisotopic hexagonal boron nitride. *Nat. Commun.* **2022**, *13*, 4347. [CrossRef] [PubMed]
179. Kianinia, M.; Regan, B.; Tawfik, S.A.; Tran, T.T.; Ford, M.J.; Aharonovich, I.; Toth, M. Robust Solid-State Quantum System Operating at 800 K. *ACS Photonics* **2017**, *4*, 768–773. [CrossRef]
180. Grosso, G.; Moon, H.; Lienhard, B.; Ali, S.; Efetov, D.K.; Furchi, M.M.; Jarillo-Herrero, P.; Ford, M.J.; Aharonovich, I.; Englund, D. Tunable and high-purity room temperature single-photon emission from atomic defects in hexagonal boron nitride. *Nat. Commun.* **2017**, *8*, 705. [CrossRef] [PubMed]
181. Dietrich, A.; Doherty, M.W.; Aharonovich, I.; Kubanek, A. Solid-state single photon source with Fourier transform limited lines at room temperature. *Phys. Rev. B* **2020**, *101*, 081401. [CrossRef]
182. Huang, Y.; Dang, Z.; He, X.; Fang, Z. Engineering of single-photon emitters in hexagonal boron nitride [Invited]. *Chin. Opt. Lett.* **2022**, *20*, 032701. [CrossRef]
183. Xiao, Y.; Yu, H.; Wang, H.; Zhu, X.; Chen, L.; Gao, W.; Liu, C.; Yin, H. Defect engineering of hexagonal boron nitride nanosheets via hydrogen plasma irradiation. *Appl. Surf. Sci.* **2022**, *593*, 153386. [CrossRef]
184. Hou, S.; Birowosuto, M.D.; Umar, S.; Anicet, M.A.; Tay, R.Y.; Coquet, P.; Tay, B.K.; Wang, H.; Teo, E.H.T. Localized emission from laser-irradiated defects in 2D hexagonal boron nitride. *2D Mater.* **2018**, *5*, 015010. [CrossRef]
185. Gao, X.; Pandey, S.; Kianinia, M.; Ahn, J.; Ju, P.; Aharonovich, I.; Shivaram, N.; Li, T. Femtosecond Laser Writing of Spin Defects in Hexagonal Boron Nitride. *ACS Photonics* **2021**, *8*, 994–1000. [CrossRef]
186. Fournier, C.; Plaud, A.; Roux, S.; Pierret, A.; Rosticher, M.; Watanabe, K.; Taniguchi, T.; Buil, S.; Quélin, X.; Barjon, J.; et al. Position-controlled quantum emitters with reproducible emission wavelength in hexagonal boron nitride. *Nat. Commun.* **2021**, *12*, 3779. [CrossRef]
187. Guo, N.-J.; Liu, W.; Li, Z.-P.; Yang, Y.-Z.; Yu, S.; Meng, Y.; Wang, Z.-A.; Zeng, X.-D.; Yan, F.-F.; Li, Q.; et al. Generation of Spin Defects by Ion Implantation in Hexagonal Boron Nitride. *ACS Omega* **2022**, *7*, 1733–1739. [CrossRef]
188. Gu, R.; Wang, L.; Zhu, H.; Han, S.; Bai, Y.; Zhang, X.; Li, B.; Qin, C.; Liu, J.; Guo, G.; et al. Engineering and Microscopic Mechanism of Quantum Emitters Induced by Heavy Ions in hBN. *ACS Photonics* **2021**, *8*, 2912–2922. [CrossRef]
189. Proscia, N.V.; Shotan, Z.; Jayakumar, H.; Reddy, P.; Cohen, C.; Dollar, M.; Alkauskas, A.; Doherty, M.; Meriles, C.A.; Menon, V.M. Near-deterministic activation of room-temperature quantum emitters in hexagonal boron nitride. *Optica* **2018**, *5*, 1128–1134. [CrossRef]
190. Sajid, A.; Ford, M.J.; Reimers, J.R. Single-photon emitters in hexagonal boron nitride: A review of progress. *Rep. Prog. Phys.* **2020**, *83*, 044501. [CrossRef] [PubMed]
191. Caldwell, J.D.; Aharonovich, I.; Cassabois, G.; Edgar, J.H.; Gil, B.; Basov, D.N. Photonics with hexagonal boron nitride. *Nat. Rev. Mater.* **2019**, *4*, 552–567. [CrossRef]
192. Li, C.; Fröch, J.E.; Nonahal, M.; Tran, T.N.; Toth, M.; Kim, S.; Aharonovich, I. Integration of hBN Quantum Emitters in Monolithically Fabricated Waveguides. *ACS Photonics* **2021**, *8*, 2966–2972. [CrossRef]
193. Elshaari, A.W.; Skalli, A.; Gyger, S.; Nurizzo, M.; Schweickert, L.; Zadeh, I.E.; Svedendahl, M.; Steinhauer, S.; Zwiller, V. Deterministic Integration of hBN Emitter in Silicon Nitride Photonic Waveguide. *Adv. Quantum Technol.* **2021**, *4*, 2100032. [CrossRef]
194. Vogl, T.; Lecamwasam, R.; Buchler, B.C.; Lu, Y.; Lam, P.K. Compact Cavity-Enhanced Single-Photon Generation with Hexagonal Boron Nitride. *ACS Photonics* **2019**, *6*, 1955–1962. [CrossRef]
195. Häußler, S.; Bayer, G.; Waltrich, R.; Mendelson, N.; Li, C.; Hunger, D.; Aharonovich, I.; Kubanek, A. Tunable Fiber-Cavity Enhanced Photon Emission from Defect Centers in hBN. *Adv. Opt. Mater.* **2021**, *9*, 2002218. [CrossRef]
196. Fröch, J.E.; Li, C.; Chen, Y.; Toth, M.; Kianinia, M.; Kim, S.; Aharonovich, I. Purcell Enhancement of a Cavity-Coupled Emitter in Hexagonal Boron Nitride. *Small* **2022**, *18*, 2104805. [CrossRef]
197. Li, X.; Scully, R.A.; Shayan, K.; Luo, Y.; Strauf, S. Near-Unity Light Collection Efficiency from Quantum Emitters in Boron Nitride by Coupling to Metallo-Dielectric Antennas. *ACS Nano* **2019**, *13*, 6992–6997. [CrossRef]
198. Peyskens, F.; Chakraborty, C.; Muneeb, M.; Van Thourhout, D.; Englund, D. Integration of single photon emitters in 2D layered materials with a silicon nitride photonic chip. *Nat. Commun.* **2019**, *10*, 4435. [CrossRef]

199. Glushkov, E.; Mendelson, N.; Chernev, A.; Ritika, R.; Lihter, M.; Zamani, R.R.; Comtet, J.; Navikas, V.; Aharonovich, I.; Radenovic, A. Direct Growth of Hexagonal Boron Nitride on Photonic Chips for High-Throughput Characterization. *ACS Photonics* **2021**, *8*, 2033–2040. [CrossRef]
200. Rahim, A.; Ryckeboer, E.; Subramanian, A.Z.; Clemmen, S.; Kuyken, B.; Dhakal, A.; Raza, A.; Hermans, A.; Muneeb, M.; Dhoore, S.; et al. Expanding the Silicon Photonics Portfolio With Silicon Nitride Photonic Integrated Circuits. *J. Light. Technol.* **2017**, *35*, 639–649. [CrossRef]
201. Xiang, C.; Jin, W.; Bowers, J.E. Silicon nitride passive and active photonic integrated circuits: Trends and prospects. *Photonics Res.* **2022**, *10*, A82–A96. [CrossRef]
202. Liu, J.; Huang, G.; Wang, R.N.; He, J.; Raja, A.S.; Liu, T.; Engelsen, N.J.; Kippenberg, T.J. High-yield, wafer-scale fabrication of ultralow-loss, dispersion-engineered silicon nitride photonic circuits. *Nat. Commun.* **2021**, *12*, 2236. [CrossRef]
203. Lu, X.; Moille, G.; Rao, A.; Westly, D.A.; Srinivasan, K. Efficient photoinduced second-harmonic generation in silicon nitride photonics. *Nat. Photonics* **2021**, *15*, 131–136. [CrossRef]
204. Liu, J.; Raja, A.S.; Karpov, M.; Ghadiani, B.; Pfeiffer, M.H.; Du, B.; Engelsen, N.J.; Guo, H.; Zervas, M.; Kippenberg, T.J. Ultralow-power chip-based soliton microcombs for photonic integration. *Optica* **2018**, *5*, 1347–1353. [CrossRef]
205. Senichev, A.; Martin, Z.O.; Peana, S.; Sychev, D.; Xu, X.; Lagutchev, A.S.; Boltasseva, A.; Shalaev, V.M. Room-temperature single-photon emitters in silicon nitride. *Sci. Adv.* **2021**, *7*, eabj0627. [CrossRef] [PubMed]
206. Xue, X.; Patra, B.; van Dijk, J.P.G.; Samkharadze, N.; Subramanian, S.; Corna, A.; Wuetz, B.P.; Jeon, C.; Sheikh, F.; Juarez-Hernandez, E.; et al. CMOS-based cryogenic control of silicon quantum circuits. *Nature* **2021**, *593*, 205–210. [CrossRef]
207. Aaronson, S.; Arkhipov, A. The computational complexity of linear optics. In Proceedings of the STOC'11: Symposium on Theory of Computing, San Jose, CA, USA, 6–8 June 2011; p. 333. [CrossRef]
208. Kumar, S.; Nehra, M.; Kedia, D.; Dilbaghi, N.; Tankeshwar, K.; Kim, K.-H. Nanodiamonds: Emerging face of future nanotechnology. *Carbon* **2019**, *143*, 678–699. [CrossRef]
209. Aslam, N.; Zhou, H.; Urbach, E.K.; Turner, M.J.; Walsworth, R.L.; Lukin, M.D.; Park, H. Quantum sensors for biomedical applications. *Nat. Rev. Phys.* **2023**, *5*, 157–169. [CrossRef] [PubMed]
210. Belser, S.; Hart, J.; Gu, Q.; Shanahan, L.; Knowles, H.S. Opportunities for diamond quantum metrology in biological systems. *Appl. Phys. Lett.* **2023**, *123*, 020501. [CrossRef]
211. Sahoo, S.; Davydov, V.A.; Agafonov, V.N.; Bogdanov, S.I. Hybrid quantum nanophotonic devices with color centers in nanodiamonds. *Opt. Mater. Express* **2023**, *13*, 191–217. [CrossRef]
212. Ngan, K.; Zhan, Y.; Dory, C.; Vučković, J.; Sun, S. Quantum Photonic Circuits Integrated with Color Centers in Designer Nanodiamonds. *Nano Lett.* **2023**, *23*, 9360–9366. [CrossRef]
213. Fu, K.-M.C.; Santori, C.; Barclay, P.E.; Beausoleil, R.G. Conversion of neutral nitrogen-vacancy centers to negatively charged nitrogen-vacancy centers through selective oxidation. *Appl. Phys. Lett.* **2010**, *96*, 121907. [CrossRef]
214. Zhang, K.; Feng, Y.; Wang, F.; Yang, Z.; Wang, J. Two dimensional hexagonal boron nitride (2D-hBN): Synthesis, properties and applications. *J. Mater. Chem. C* **2017**, *5*, 11992–12022. [CrossRef]
215. You, L. Superconducting nanowire single-photon detectors for quantum information. *Nanophotonics* **2020**, *9*, 2673–2692. [CrossRef]
216. Kambs, B.; Becher, C. Limitations on the indistinguishability of photons from remote solid state sources. *New J. Phys.* **2018**, *20*, 115003. [CrossRef]
217. Sipahigil, A.; Jahnke, K.D.; Rogers, L.J.; Teraji, T.; Isoya, J.; Zibrov, A.S.; Jelezko, F.; Lukin, M.D. Indistinguishable Photons from Separated Silicon-Vacancy Centers in Diamond. *Phys. Rev. Lett.* **2014**, *113*, 113602. [CrossRef]